European Journal of Operational Research 305 (2023) 1194–1214

Contents lists available at ScienceDirect

European Journal of Operational Research

journal homepage: www.elsevier.com/locate/ejor

Production, Manufacturing, Transportation and Logistics

Matching functions for free-floating shared mobility system optimization to capture maximum walking distances☆

Matthias Soppert[a,*], Claudius Steinhardt[a], Christian Müller[b], Jochen Gönsch[b], Prasanna M. Bhogale[c]

[a] Chair of Business Analytics & Management Science, University of the Bundeswehr Munich, Germany
[b] Chair of Service Operations, Mercator School of Management, University of Duisburg-Essen, Germany
[c] SHARE NOW, Berlin

ARTICLE INFO

Article history:
Received 1 September 2021
Accepted 28 June 2022
Available online 4 July 2022

Keywords:
Transportation
Free-floating shared mobility systems
Modeling
Matching functions
Optimization

ABSTRACT

Shared mobility systems have become a frequently used inner-city mobility option. In particular, free-floating shared mobility systems are experiencing strong growth compared to station-based systems. For both, many approaches have been proposed to optimize operations, e.g., through pricing and vehicle relocation. To date, however, optimization models for free-floating shared mobility systems have simply adopted key assumptions from station-based models. This refers, in particular, to the models' part that formalizes how rentals realize depending on available vehicles and arriving customers, i.e., how supply and demand match. However, this adoption results in simplifications that do not adequately account for the unique characteristics of free-floating systems, leading to overestimated rentals, suboptimal decisions, and lost profits.

In this paper, we address the issue of accurate optimization model formulation for free-floating systems. Thereby, we build on the state-of-the-art concept of considering a spatial discretization of the operating area into zones. We formally derive two novel analytical matching functions specifically suited for free-floating system optimization, incorporating additional parameters besides supply and demand, such as customers' maximum walking distance and zone sizes. We investigate their properties, like their linearizability and integrability into existing optimization models. Our computational study shows that the two functions' accuracy can be up to 20 times higher than the existing approach. In addition, in a pricing case study based on data of Share Now, Europe's largest free-floating car sharing provider, we demonstrate that more profitable pricing decisions are made. Most importantly, our work enables the adaptation of station-based optimization models to free-floating systems.

1. Introduction

Shared mobility systems (SMSs) such as car sharing and bike sharing systems have become an integral part of the inner-city mobility. Globally, the shared mobility market today has a size of approximately 250 bn. USD and is projected to grow annually by around 25% the next years (Data Bridge Market Research, 2021). Among the two general concepts of free-floating (FF) and station-based (SB) systems (Lu, Chen, & Shen, 2017), especially FF SMSs experienced considerable growth during the last decade (Shaheen, Cohen, & Jaffee, 2018). The decisive difference between FF SMSs and SB SMSs is that pick-up and drop-off locations for vehicles are not limited to certain predefined locations – the *stations* in an SB SMS. Instead, in an FF SMS, vehicles are *free-floating* within some predefined operating area and can be dropped-off (and picked-up) at any publicly accessible location.

The optimization of SMSs, e.g. with regard to pricing and relocation, has been studied extensively in the literature, summarized e.g. in review papers on car sharing by Ferrero, Perboli, Vesco, Caiati, & Gobbato (2015a) and on SMSs in general by Laporte, Meunier, & Wolfler Calvo (2018), Ataç, Obrenović, & Bierlair (2021). However, in the body of works addressing operational optimization problems with endogenous modeling of rentals, FF SMSs –

☆ This work was supported by the University of the Bundeswehr Munich.
* Corresponding author.
E-mail addresses: matthias.soppert@unibw.de (M. Soppert), claudius.steinhardt@unibw.de (C. Steinhardt), christian.mueller.9@uni-due.de (C. Müller), jochen.goensch@uni-due.de (J. Gönsch), prasanna.bhogale@share-now.com (P.M. Bhogale).

https://doi.org/10.1016/j.ejor.2022.06.058

despite their dominance in practice – have not been adequately considered. Instead, up to now, FF SMSs are treated like SB SMSs (compare e.g. Haider, Nikolaev, Kang, & Kwon, 2018; Jorge, Molnar, & Correia, 2015 for SB SMSs and Hardt & Bogenberger, 2021; Lu, Correia, Zhao, Liang, & Lv, 2021 for FF SMSs). However, as it turned out in a close collaboration with Share Now, Europe's largest FF car sharing provider operating in 16 cities in 8 countries (Share Now, 2021), ignoring the difference between both concepts in the optimization models can result in an overestimation of rentals in the FF SMS, suboptimal decisions and substantial profit losses. In this work, we address and solve this fundamental issue of inaccurate rentals modeling in FF SMS optimization models.

To give an idea of the causes of this issue, we first need to consider how SMS optimization models are usually formulated: Regarding space, it is the state-of-the-art approach in literature and practice to discretize the operating area of an FF SMS into *zones* – the counterpart of *stations* in an SB SMS (e.g. Neijmeijer, Schulte, Tierney, Polinder, & Negenborn, 2020; Weikl & Bogenberger, 2016). Regarding time, the considered time frame is discretized into *periods* for both SB and FF SMSs. The SMSs are described and optimized on this level of aggregation, i.e. relevant data (e.g. demand) is collected, and optimization models are formulated on this *location*-period level (station-period in SB SMSs, zone-period in FF SMSs). Typically, these optimization models are mixed-integer (linear) programs based on network flow formulations for both SB (e.g. Jorge et al., 2015) and FF (e.g. Lu et al., 2017) SMSs.

Now, a central component of these optimization models is the formalization on the location-period level how rentals realize in dependence of the number of available vehicles and the number of arriving customers – i.e., how supply and demand *match*. The existing SB and FF SMS optimization models rely on the implicit assumption that rentals are determined by the *minimum of supply and demand*. While the realization of rentals can be modeled well with this *matching function* in an SB SMS, applying the same simplified assumption to FF SMSs can cause substantial errors. Consider e.g. a *station*-period combination in an SB SMS with one (expected) available vehicle and one (expected) arriving customer. In this SB SMS, it is valid to assume that one (expected) rental realizes. For the same situation in an FF SMS in contrast, an accurate matching function must differ: When the zone is large, the available vehicle is not necessarily within reach of the customer, because the *zone* has a spatial expansion and customers have a maximum willingness-to-walk (e.g. Herrmann, Schulte, & Voß, 2014). Thus, *at most* one – for a large zone, much less than one – (expected) rental results. Note that we explicitly write "(expected)", because even though realizations of supply, demand and rentals are discrete values in reality, they can be (and often are) *modeled* continuously.

A presumably simple solution is to apply a finer spatial discretization scheme to the FF SMS, i.e. to define many small zones such that a customer can reach any vehicle in the respective zone, and then use the matching function to determine rentals as in an SB SMS. This, however, simply substitutes the problem of a vehicle being too far away in a large zone by other problems, which become more severe with decreasing zone size: Most importantly, defining many small zones is problematic, because observed data points of demand and supply that in reality resulted in a rental are more likely to be assigned to neighboring zones such that there would not be a matching in the FF SMS model. This aggregation error is related to the *modifiable areal unit problem* (see, e.g., Manley, 2019) which summarizes that statistical results, such as mean values, variance, and correlations do depend on the specific discretization scheme. Typical discretization schemes in literature and practice use zones in the order of several square kilometers (e.g. Weikl & Bogenberger, 2016) and for these zone area sizes, the described issue regarding the supply-demand matching due to the customers' maximum walking distance indeed prevails. These larger zone area sizes also have the practical advantage that the typically resulting fifty to hundred zones have a count which is still manageable for the staff of the SMS provider and that the optimization models which scale with the zone count do not grow too large. All of the named aspects already show that the decision on appropriate discretization schemes (including count, size and shape of zones) for FF SMSs is very complex. In fact, there is no single best definition of the discretization scheme. Thus, in our work, we consider a certain discretization scheme *as given*, and we address the search for accurate matching functions for FF SMSs that adapt to the given circumstances.

Clearly, any matching process can be replicated arbitrarily exact with stochastic simulations that consider discrete supply, demand, and resulting rentals. However, we are interested in *analytical* functions that output expected rentals (continuous values) and that can be integrated in the existing SMS optimization models from the literature. Therefore, to solve the issue of inaccurate matching modeling in FF SMS optimization models, we first formulate a general matching function that replicates the matching process within an FF SMS and incorporates its specific characteristics. Based on this, we then formally derive two novel matching functions which are specifically suited for FF SMS optimization models. We also formalize what is assumed in the existing literature so far by a third matching function and show that only the two novel matching functions can widely be applied to FF SMSs, and that their integration in FF SMS optimization models improves decision making.

To properly distinguish our work from the literature, two streams are of particular importance. First, matching functions have a long history in *macroeconomics*, mostly focusing on labor markets and with the intention to explain unemployment (e.g. Petrongolo & Pissarides, 2001). Some extensions also consider matching functions in transportation systems, such as taxi systems (e.g. Buchholz, 2019). However, as we discuss in more detail in Section 2, matching functions that incorporate the specifics of FF SMSs have not been discussed yet. Moreover, in contrast to this literature stream, our focus eventually lies on the formulation of optimization models, such that we have a different view on matching functions and their requirements: For example, the matching functions' linearizability and integrability in an overall FF SMS optimization model is of particular importance in our case, but irrelevant in the existing literature. Second, the development of *matching functions* for FF SMSs in our work must not be mixed up with the development of so-called *matching algorithms* in *platform-based SMSs* such as *on-demand ride-hailing*, like Uber or Lyft (e.g. Yan, Zhu, Korolko, & Woodard, 2020). In the latter, a *central platform* faces the problem to *assign* customer requests most efficiently to available drivers. Since the customer's GPS coordinates are shared with the driver after the assignment happened, the ride realizes with certainty and, thus, there is no need for *matching functions* in the sense explained above. In contrast to the matching algorithms in platform-based SMSs, the provider of the SMSs that we consider *cannot explicitly* decide on the *assignment* of vehicles to customers as customers choose vehicles themselves. Instead, the *matching functions* formalize how many rentals are expected to realize within some location-period combination, given supply, demand, and other relevant parameters.

The contributions of this paper are as follows:

- To the best of our knowledge, we are the first to reveal the necessity to formulate SB and FF SMS optimization models differently. We show that more sophisticated matching functions improve FF SMSs models and the decisions resulting from optimization.

- Second, we derive two novel matching functions for FF SMSs, which take into account the customers' sequential arrival, their maximum walking distance, and the size of the zone. These functions differ regarding their mathematical properties and can be integrated in different types of optimization models – one into the widespread linear network flow-based SMS optimization models, allowing to adapt a variety of existing SB SMS optimization models to FF SMSs.
- Third, we formalize a third matching function that reflects the assumptions made (implicitly) in the SMS optimization literature, i.e. that (expected) rentals correspond to the minimum of (expected) supply and demand. We demonstrate that this benchmark does not yield accurate rentals estimations for FF SMSs in general. Our analytical investigation of this function's properties shows that this shortcoming cannot be remedied by artificially partitioning zones for which data is given into multiple smaller zones.
- Fourth, in a computational study, we demonstrate that the rental prediction accuracy of the novel functions in an FF SMS is substantially higher than the benchmark function. This is because the novel matching functions adapt to the given circumstances, in particular to different zones sizes.
- Fifth, in a case study based on real-life data, we integrate one of the novel matching functions into an existing pricing optimization framework and demonstrate significant profit increases that can be ascribed solely to the more accurate matching modeling.

Overall, this work primarily contributes to the literature on FF SMS optimization from the operations research stream of literature. We build a bridge between the optimization of SB and FF SMSs, in the sense that, by the approaches presented in this paper, existing optimization approaches that were specifically designed for SB SMSs can straightforwardly be generalized to make them applicable for FF SMSs as well.

The remainder of the paper is structured as follows. In Section 2, we review the related literature. Section 3 discusses the novel as well as the benchmark matching functions. Section 4 contains the numerical study considering the rentals prediction accuracy. In Section 5, we assess the importance of accurate matching modeling in optimization problems by considering a pricing optimization case study. Section 6 covers managerial insights, concludes the paper and gives an outlook.

2. Literature

The literature on SMS optimization is broad and covers decision making at strategic, tactical and operational levels (Laporte et al., 2018). Various review papers on bike sharing (DeMaio, 2009; Fishman, Washington, & Haworth, 2013; Ricci, 2015) and car sharing (Brendel & Kolbe, 2017; Ferrero et al., 2015a; Ferrero, Perboli, Vesco, Musso, & Pacifici, 2015b; Golalikhani, Oliveira, Carravilla, Oliveira, & Antunes, 2021a; Golalikhani, Oliveira, Carravilla, Oliveira, & Pisinger, 2021b; Illgen & Höck, 2019; Jorge & Correia, 2013) summarize the literature. Our work contributes to the tactical (e.g. fleet sizing) and operational (e.g. relocation or pricing) levels where matching functions are (implicitly) used and, as we will see, more advanced matching functions are required for FF SMSs.

Until now, matching functions for SMSs and the necessity of modeling FF SMSs differently than SB SMSs has not been discussed in the literature. On the contrary, the literature is divided on whether *any* differences need to be made between optimization models of SB and FF SMSs and we explore these views in Section 2.1. In Section 2.2, we provide an overview on SMS optimization problems with a focus on the wide spread approaches formulated as time-expanded networks. These works are relevant because existing assumptions regarding matching can be concluded from their optimization models and these works are the ones where our novel matching functions can be integrated in. In Section 2.3, we review the literature on matching functions from macroeconomics. In Section 2.4, we briefly review two other related literature streams, namely agent-based FF SMS simulations and empirical studies, as these works implicitly provide insights regarding relevant parameters for matching functions.

Note that, as explained in Section 1, we do not consider *platform-based* mobility offers like on-demand ride-hailing that *assign* customer requests to vehicles (e.g. Boysen, Briskorn, & Schwerdfeger, 2019; Yan et al., 2020), because the nature of these problems differs fundamentally from those in the SMSs that we consider (car sharing etc.).

2.1. Station-Based vs. free-floating shared mobility system optimization

SB SMSs have a relatively long history in practice – the first SB car sharing system was installed in 1948 in Switzerland (called Sefage) (Shaheen, Sperling, & Wagner, 1998). In contrast, the concept of FF SMSs, which today largely relies on the usage of mobile phones and GPS tracking only became technically realizable much later and arguably was first put into practice with an FF car sharing system in 2008 in Germany (Ciari, Bock, & Balmer, 2014) (called car2go which ten years later became Share Now). This temporal delay of FF SMSs is reflected in the literature, where the majority of papers consider SB SMSs. For example, in the general survey paper on SMSs, Laporte, Meunier, & Wolfler Calvo (2015) entirely focus on SB SMSs, while their updated survey a few years later explicitly differs between SB and FF SMSs (Laporte et al., 2018).

Regarding the optimization of these SMSs, there are different views in the literature on whether SB and FF SMSs can be considered identical or not: Some authors state that SB and FF SMSs can be treated *identically*. As stated in Section 1, this view is based on the fact that the state-of-the-art approach in literature and practice regarding the modeling of FF SMSs is to discretize the operating area into zones (e.g. Neijmeijer et al., 2020; Weikl & Bogenberger, 2016). Thus, it is tempting to equate stations and zones. For example, in their review paper on relocations in one-way car sharing, Illgen & Höck (2019) argue that "free-floating operation areas are usually partitioned into smaller zones that serve as virtual stations, such that the VReP [vehicle relocation problem] can be applied perfectly for relocations that occur between those zones instead of from station to station". Similarly, Lu et al. (2021) who consider combined relocation and pricing on the performance of one-way car sharing systems, implicitly state that SB and FF SMSs can be considered identically, as they use the decisive terms "stations" and "zones" interchangeably.

The only researchers we know of who represent a *more differentiated* view are from Bogenberger's group. Weikl & Bogenberger (2015) e.g. consider relocation optimization for FF SMSs. On the one hand, they state that from a technical viewpoint, SB SMS optimization models can be transferred to FF SMSs by "dividing the operating area into station-like zones." On the other hand, they state that "transferring the existing relocation models for station-based systems to free-floating car sharing systems is however restricted" and they give multiple reasons related to the considered relocation problem (see also Weikl & Bogenberger, 2013). The authors e.g. argue that zone-level relocation decisions are not specific enough for FF SMSs because vehicles have specific positions. Another argument concerns the optimization model, since zones of FF SMSs "do not have strict capacity limits" in contrast to stations in SB SMSs. To address these issues, the authors define "macroscopic zones" which are separated into "microscopic zones". The relocation decisions on macroscopic level are determined by optimiza-

tion while the decisions on microscopic level are rule-based. Note that in the models of Weikl & Bogenberger (2013) and Weikl & Bogenberger (2015), the issue of accurate matching modeling does not arise, because the optimal number of vehicles per zone which is affected by the relocation decisions is given and rentals are not modeled endogenously (see also Section 2.2).

In our work, we demonstrate that SB and FF SMS optimization models indeed need to differ. While Weikl & Bogenberger (2015) focus on relocation, in this paper we address the essential issue of matching modeling, which is necessary for all optimization models in which rentals are endogenously modeled. We in particular show that once that data is collected on some defined zone level, artificially subdividing this zone into multiple sub-zones which correspond to stations of an SB SMS does not address the issue of inaccurate rentals predictions (Section 3).

2.2. Network flow-based shared mobility system optimization models

The dynamically changing, imbalanced distribution between available and demanded vehicles is a well-known challenge of SMSs (Jorge & Correia, 2013; Lippoldt, Niels, & Bogenberger, 2019; Molnar & Correia, 2019). Most tactical and operational optimization approaches seek to address this problem in order to optimize for the actual service- or monetary-related goal. To that end, the proposed approaches typically consider the interaction of supply and demand over the entire SMS by modeling the system with a time-expanded network, where rentals and relocations are described by flows. Note that not all network flow-based SMS models consider rentals *endogenously*. For example, papers on relocation typically consider the desired number of vehicles at different spatio-temporal network nodes as given, and model only the operator-based vehicle movements (=relocations) to serve this demand as network flows. The matching functions in this work determine the user-based vehicle movements (=rentals) in dependence of supply, demand and other parameters. Accordingly, they are only relevant for optimization models with endogenous rentals which we focus on in the following.

Among these works, we identify three groups. First, works that consider SB SMSs (e.g. Haider et al., 2018; Jorge et al., 2015), second, works that consider FF SMSs (e.g. Hardt & Bogenberger, 2021; Lu et al., 2017; Lu et al., 2021), and third, works that consider SMSs in general (e.g. Correia & Antunes, 2012; Soppert, Steinhardt, Müller, & Gönsch, 2022), by speaking of *locations* instead of *stations* or *zones*. Among the first and second group, several works do not use the term *station-based* or *free-floating* explicitly, but their problem description and modeling where they use the terms *station* or *zone* allows to classify them.

To the best of our knowledge, the issue of supply and demand matching in FF SMSs has not been addressed in any of these works, or elsewhere in the literature. Still, the above works model the relation between supply, demand, and rentals, such that assumptions regarding the matching modeling within a specific location-period are implicitly revealed: All of the above-named works use the concept that rentals are the minimum of demand and supply. Other parameters that may affect the matching are not considered. To the best of our knowledge, there are only two works in the above-named groups (Hardt & Bogenberger, 2021; Soppert et al., 2022) that explicitly model (expected) rentals to *equal* the minimum of (expected) supply and (expected) demand (always add "(expected)" in the following). All other works formulate constraints that only *limit* rentals to this minimum because they propose optimistic optimization models in the sense that the operator can deny a rental although there is supply and demand (see Soppert et al., 2022 for further discussions).

To summarize the SMS literature regarding matching modeling, one can conclude from the optimization models that it is current practice to (explicitly or implicitly) assume that rentals are determined by the minimum of supply and demand and this simplistic assumption is applied to both SB and FF SMSs. With regard to the three groups in the literature identified above, our contribution is to develop matching functions that allow to apply SB SMS models to FF SMS models (first group) and to improve FF and unspecified SMS models (second and third group).

Even if supply and demand matching has not been considered explicitly, the above works impose requirements on the matching functions that we develop. For one thing, the matching functions need to be compatible with a spatio-temporal discretization and shall be seamlessly integratable into these SMS models. More specifically, the matching functions' in- and output need to be compatible with the overall SMS models from literature. For another, many approaches are formulated as linear optimization problems. Therefore, linear matching functions that retain the linearity of the overall model have an additional value for the generalizability of existing literature.

2.3. Matching functions

Analytical formulations that describe the formation of new relationships, i.e. *matches*, from unmatched agents are denoted as (*aggregate*) *matching functions* and have originally been discussed in macroeconomics, often in the context of stylized (labor) markets. The motivation to formulate these matching functions is to explain "coordination failures" that e.g. "explain the existence of unemployment" (despite job availability) through "the modeling of *frictions*" which derive e.g. from "information imperfections" or "heterogeneities" (Petrongolo & Pissarides, 2001). In their survey paper on matching functions, Petrongolo & Pissarides (2001) state that for labor markets the simplest matching function m is of the form $M = m(U, V)$, where M is the number of jobs that result during a given time interval in dependence of unemployed workers U and vacant jobs V. Different underlying mechanisms of the matching process, called *microfoundations*, are assumed that lead to different matching functions. For example, the earliest works by Butters (1977) and Hall (1979) formulate matches based on an urn-ball microfoundation, where (in labor market context) workers randomly send applications (balls) to job vacancies (urns). Under the simplest assumption that "U workers know exactly the location of job V vacancies", that workers "send one application each", and that "a vacancy [...] selects an applicant at random", the resulting matching function becomes $M = V \cdot [1 - (1 - 1/V)^U]$ which can be approximated by $M = V \cdot [1 - e^{-U/V}]$ (Petrongolo & Pissarides, 2001).

In the context of transportation, the matching between customers and drivers in taxi systems has been analyzed by Bian (2018), Buchholz (2019), Fréchette, Lizzeri, & Salz (2018) as well as Ata, Barjesteh, & Kumar (2019). The matching functions of the first two are based on the works named above, have the same structural form, and are only slightly modified, e.g. by a "location specific parameter" (Bian, 2018) that allows to calibrate to spatial heterogeneities. A particular matching function that holds "in the absence of frictions" is $M = \min(U, V)$ (Petrongolo & Pissarides, 2001), also denoted as "perfect matching" (Bian, 2018) or "frictionless matching" (Buchholz, 2019), which in the latter is used to describe the search process by taxis for customers at airports.

In contrast, Fréchette et al. (2018) as well as Ata et al. (2019) use fundamentally different approaches to derive matching functions for taxi systems. Fréchette et al. (2018) picture different areas of a city where each area consists of a grid of locations that represent street corners. A matching function is approximated through a simulation in which customers and drivers appear randomly on these locations. Customers wait for some time before they leave and whenever a driver arrives at a location where a

customer is waiting a match realizes. Ata et al. (2019) propose an analytical approach in which they draw the number of customers and drivers each from a Binomial distribution and then derive the expected number of matches by taking the minimum of both values. To find a tractable approximation, the authors use the Normal distribution and linear approximations to obtain the eventual matching function.

To the best of our knowledge, matching functions for FF SMSs have not yet been discussed in the literature. In our work, we fill this gap by deriving matching functions which are based on FF SMSs specifics (*microfoundations*), such as zone sizes and customers' willingness-to-walk. These parts of our work contribute to the matching functions literature. However, since we focus on FF SMS *optimization* – during development of the functions as well as in a pricing optimization case study – we overall see our contribution with regard to the SMS optimization literature from operations research. E.g. other than in the matching function literature, additional properties for the newly developed functions, like e.g. the integrability into optimization models, are of particular interest in our work. In Section 3, we establish the connection between the developed matching functions and literature and e.g. discuss under which conditions the frictionless matching mentioned above can be applied to FF SMSs.

2.4. Further related literature streams

The first related literature stream uses agent-based simulations to derive insights on SMSs. Typical applications are e.g. the evaluation of SMSs within a multi-commodity transportation network (Ciari, Balac, & Axhausen, 2016; Heilig, Mallig, Schröder, Kagerbauer, & Vortisch, 2018; Li, Liao, Timmermans, Huang, & Zhou, 2018), the impact of specific (parking) pricing rules (Balac, Ciari, & Axhausen, 2017; Ciari, Balac, & Balmer, 2015), or the interplay of competing SMS providers (Balac, Becker, Ciari, & Axhausen, 2019). Because of the system's description on agent level, including customer behavior and exact vehicle positioning, matching is indeed considered in these simulations. However, an analytical formalization of the matching, in particular on location-period level, as required for the integration into network flow-based optimization problems, is not given. Another application of agent-based simulations is to serve as a heuristic solution approach for network flow optimization problems that we consider in our work (see e.g. Cocca, Giordano, Mellia, & Vassio, 2019), but also in this case no analytical formulations of the matching is provided.

The second related literature stream deals with empirical studies on FF SMS. These works provide requirements for and relevant parameters of suitable matching functions. From several studies one can conclude that matching functions have to consider spatio-temporal differences of an SMS. For example, Reiss & Bogenberger (2016) simulate a bike sharing system based on empirical data and identify different demand patterns for weekdays and weekends, as well as for different locations and times of the day. Hardt (2018) also reports different spatio-temporal demand patterns and furthermore identifies differences regarding the resulting rentals, drop-offs, and availabilities within the operating area. Regarding relevant parameters on the customers' decision for the matching functions in FF SMSs, literature especially mentions the distance/walking time to the vehicles as well as the pricing. For example, Wu, Le Vine, Sivakumar, & Polak (2019) investigate the user behavior with a stated-choice experiment considering for example walking time, willingness to pay, and socio-demographical features. Niels & Bogenberger (2017) analyze app openings and booking data from a car sharing system. Among other results, they report a high influence of the distance to available vehicles on the customers' decision.

3. Modeling rentals in FF SMS optimization problems

In this section, we propose and discuss two novel analytical matching functions to model rentals in FF SMS optimization problems. Further, we formalize a third one which reflects the matching as it is currently assumed in the SMS optimization literature and which will serve as a benchmark later in the computational study. In Section 3.1, we begin by discussing the required output as well as reasonable inputs for the matching functions. Section 3.2 presents a generic stylized matching process and a corresponding generic matching function on which all specific matching functions are based. In Section 3.3, we systematically derive the different functions, along with their specific underlying assumptions. Section 3.4 discusses mathematical properties and Section 3.5 the potential of being integrated into linear optimization problems for each of the matching functions.

3.1. Output and inputs

We begin by stating the *output* of the matching functions: As discussed in Sections 1 and 2.2, SMS optimization models are typically formulated based on network flow formulations, consisting of multiple locations and periods. In these SMS models, vehicle movements, i.e., rentals and relocations, have a certain location-period origin as well as a certain location-period destination. To fit in these network flow SMS models, a compatible matching function's output simply needs to quantify the (expected) number of rentals r that originate in a certain location and period. Conversely, it is not determined by the matching function how the rentals that realize in a specific origin split into different destinations, as this can be covered by other components of the overall SMS network flow model (see Section 3.5).

We continue with stating reasonable *inputs* for the matching functions: Clearly, the rentals depend on the number of available vehicles and arriving customers in a given location and period. Therefore, these quantities, which we denote as a and d, are inputs. However, when considering the realization of rentals in an FF SMS, two additionally necessary parameters become immediately apparent, namely the maximum distance that customers are willing to walk and the size of the zone. With a maximum walking distance in the order of several hundred meters (e.g. Herrmann et al., 2014; Niels & Bogenberger, 2017), and a typical zone size of several square kilometers (e.g. Müller, Correia, & Bogenberger, 2017; Weikl & Bogenberger, 2016), it is clear that an available vehicle is not necessarily within reach of a customer, even if the customer and vehicle are in the same zone. In order to formalize the matching functions based on these two additional parameters, we define A_w as the size of the area within walking distance and A_z as the size of the zone. The matching functions therewith become a function of the discussed inputs and parameters, meaning $r = r_{A_w,A_z}(a,d)$.

3.2. Preliminaries: Generic matching

3.2.1. Stylized matching process

As discussed above, matching functions for network flow-based SMS optimization models require to describe the rentals r on *location-period level*, given a and d. In contrast, the actual matching process in reality is independent of the artificial spatio-temporal discretization and underlies dynamics that take place *within* the period. In this section, we therefore introduce a stylized matching process that considers the requirements imposed by the discretization in the SMS model as well as the intent to formalize analytical functions that replicate the real matching process as accurately as possible. We take the following as-

sumptions for the stylized matching process on location-period level:

- All vehicles a become available *at the beginning* and customers d arrive sequentially *during* the period. More precisely, the a vehicles are first distributed over the zone. Second, the d customers arrive sequentially and potentially rent one of the vehicles each. Both a and d have zero variance, meaning that these are deterministic values in the matching process. We assume homogeneity of the zone, such that the exact locations of vehicles and customers are drawn from a uniform distribution. To formalize the process and in particular its intermediate states, we denote the *remaining* customers to arrive during a period as $\hat{d}$ and the remaining available vehicles as $\hat{a}$.
- Each of the remaining available vehicles belongs to a corresponding part of the zone, meaning that the vehicle would be within reach for an arriving customer from this part. We say that a vehicle *covers* a part of the zone area and we denote the size of the area that is covered by $\hat{a}$ vehicles all together as $A_{\hat{a}}$. The size of the marginally covered area by the $\hat{a}$th vehicle is denoted as $\Delta A_{\hat{a}}$. The matching functions differ in their assumption how the vehicles are spatially distributed and how additional vehicles cover additional parts of the zone.

Note that it is reasonable to define the marginal coverage of a *vehicle* $\Delta A_{\hat{a}}$ in dependence of the walking area A_w of a *customer*: As stated above, we assume homogeneity of a zone such that the probability of any location within the zone to lie within A_w is equal. Considering a situation with one available vehicle, the probability that this vehicle is located within the reachable area of the customer A_w is equivalent to the probability that the customer arrival location lies within the area A_w which is covered by the vehicle. The latter is in line with the assumption that vehicles are available from the beginning of a period and that customers arrive sequentially.

- For every arriving customer, there is a certain probability that a rental realizes. Clearly, this probability depends on the remaining available vehicles $\hat{a}$ in the zone, the customer's walking area A_w as well as the zone area size A_z. Since $\hat{a}$ and therewith $A_{\hat{a}}$ may change over the matching process, also this matching probability, which we denote by $P_{A_w,A_z}(\hat{a})$, generally differs for each of the customers. We assume that a rental realizes if the customer arrival position lies within the (currently) covered zone area $A_{\hat{a}}$. Considering the uniform distribution for a customer's exact arrival position, the probability of a matching $P_{A_w,A_z}(\hat{a})$ therewith is equal to the proportion of the covered area to the entire zone area, meaning $P_{A_w,A_z}(\hat{a}) = \frac{A_{\hat{a}}}{A_z}$. The matching process ends if all customers have arrived or if all vehicles have been rented.

Note that drawing exact positions from the uniform distribution corresponds to assuming homogeneity of the zone. We define a zone as the smallest considered spatial unit within an FF SMS for which data is aggregated or given. This implies that no information on a more disaggregate level is available which would justify separating a (heterogeneous) zone into multiple (homogeneous) ones. Later, in the numerical study, we vary the zone size which corresponds to different given levels of spatial data aggregation and we evaluate the matching functions with regard to their adaptability to these different circumstances.

3.2.2. Generic matching function

Given the above assumptions, the matching process within a location-period combination can be formalized by the following generic matching function

$$r_{A_w,A_z}(\hat{a},\hat{d}) = P_{A_w,A_z}(\hat{a}) \cdot (1 + r_{A_w,A_z}(\hat{a}-1,\hat{d}-1)) + (1 - P_{A_w,A_z}(\hat{a})) \cdot r_{A_w,A_z}(\hat{a},\hat{d}-1) \qquad \forall \hat{a},\hat{d} \in \mathbb{Z} \quad (1a)$$

$$r_{A_w,A_z}(\hat{a},0) = 0 \qquad \forall \hat{a} \in \mathbb{Z} \quad (1b)$$

$$r_{A_w,A_z}(0,\hat{d}) = 0. \qquad \forall d \in \mathbb{Z} \quad (1c)$$

The inter-dependencies between the possible rental realizations and the changing zone coverages are formulated by a recursion over the customer arrivals (1a). For every arriving customer, the probability that a rental realizes is $P_{A_w,A_z}(\hat{a})$. In case of a match, one rental is counted and the number of available vehicles is reduced by one. With probability $\bar{P}_{A_w,A_z}(\hat{a}) = 1 - P_{A_w,A_z}(\hat{a})$, no rental takes place such that the subsequent customer (if existent) has the same number of vehicles available, i.e. $\hat{a}$. Independent of the outcome, the number of customers to come is reduced by one, i.e. $\hat{d} \leftarrow \hat{d} - 1$. The boundary conditions (1b) and (1c) ensure that the number of rentals is zero if either supply or demand are zero. Note that (1) is a discrete function in $\hat{a}$ and $\hat{d}$ but that its output of *expected* rentals in general takes continuous values. In reality, of course, realizations of supply, demand, and rentals are discrete but since matching functions, meaning (1) as well as all introduced in the following, are *models* that aim at replicating reality, continuous outputs are reasonable or even desired if interpreted as expected values (see Section 3.5).

In the context of an overall network flow SMS model, (1) would then be integrated to calculate the resulting rentals for a specific location-period combination with corresponding vehicle count a and arriving customers d, i.e., by evaluating $r_{A_w,A_z}(a,d)$.

3.3. Derivation of matching functions

Based on the previously described generic matching process, we derive three matching functions in this section. The decisive difference between the functions is the rate with which an additional vehicle covers the area of the zone. Consequently, we denote the three functions as

- *degressive coverage rate* matching function (DCR) (Section 3.3.1),
- *constant coverage rate* matching function (CCR) (Section 3.3.2), and
- *infinite coverage rate* matching function (ICR) (Section 3.3.3).

The assumptions of the DCR come closest to the real matching process, but also the other two functions, especially the CCR, have a range of validity, and other advantages compared to the DCR.

3.3.1. The degressive coverage rate matching function (DCR)

The DCR results from the generic matching function (1) by further specifying the matching probability $P_{A_w,A_z}(\hat{a})$. The underlying assumption of the DCR is that each part of the zone is equally likely to belong to the area covered by a vehicle. Thus, the area covered by an additional vehicle comprises a part that is newly covered (marginally covered area) and a part that is already covered by the other vehicles (and wasted in this sense). More formally, the DCR assumes that, for a given available vehicle count $\hat{a}$, the additionally covered area $\Delta A_{\hat{a}+1}$ by one additional vehicle, meaning by the $(\hat{a}+1)^{st}$ vehicle, is a fraction of A_w. This fraction is the ratio of the not covered zone area with $\hat{a}$ vehicles $\bar{A}_{\hat{a}} = A_z - A_{\hat{a}}$ to the entire zone area, meaning $\Delta A_{\hat{a}+1} = A_w \cdot \frac{\bar{A}_{\hat{a}}}{A_z}$.

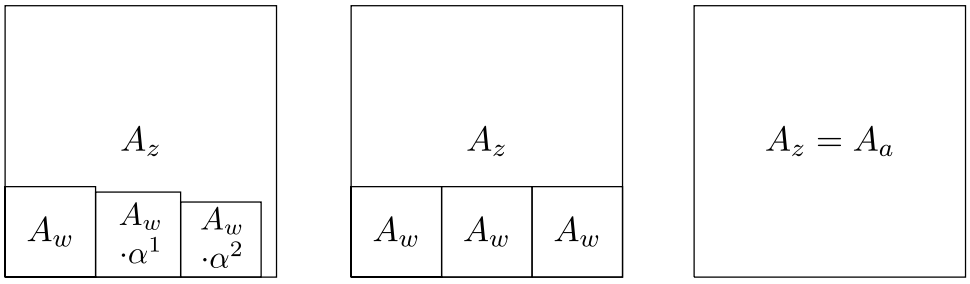

(a) DCR, $\alpha = (1 - \frac{A_w}{A_z})$, $A_{a=3} = A_w \cdot (1 + \alpha + \alpha^2)$

(b) CCR, $\lambda = \mu = 1$, $A_{a=3} = 3 \cdot A_w$

(c) ICR, $A_{a \geq 1} = A_z$

Fig. 1. Illustrative representation of coverage by matching functions.

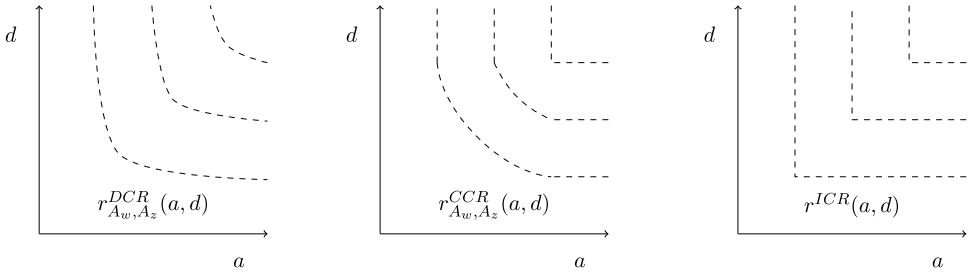

(a) DCR (b) CCR (c) ICR

Fig. 2. Schematic iso-rental curves for different matching functions and a specific A_w, A_z with $A_w < A_z$.

Proposition 1. *Assuming* $\Delta A_{\hat{a}+1} = A_w \cdot \frac{\bar{a}_a}{A_z}$, *the matching probability is* $P_{A_w,A_z}(\hat{a}) = (1 - (1 - \frac{A_w}{A_z})^{\hat{a}})$ *and the DCR is defined by*

$$\textbf{DCR:} \quad r^{DCR}_{A_w,A_z}(\hat{a},\hat{d}) = (1 - (1 - \frac{A_w}{A_z})^{\hat{a}}) \cdot (1 + r^{DCR}_{A_w,A_z}(\hat{a}-1,\hat{d}-1))$$
$$+ \left(1 - \frac{A_w}{A_z}\right)^{\hat{a}} \cdot r^{DCR}_{A_w,A_z}(\hat{a},\hat{d}-1) \qquad \forall \hat{a},\hat{d} \in \mathbb{Z} \qquad (2a)$$

$$r^{DCR}_{A_w,A_z}(\hat{a},0) = 0 \qquad \forall \hat{a} \in \mathbb{Z} \qquad (2b)$$

$$r^{DCR}_{A_w,A_z}(0,\hat{d}) = 0. \qquad \forall \hat{d} \in \mathbb{Z} \qquad (2c)$$

We prove Proposition 1 in Appendix B. Figure 1a illustrates the marginal coverage of the DCR for $a = 3$ vehicles. The $\hat{a}$th vehicle additionally covers $A_w \cdot (1 - \frac{A_w}{A_z})^{\hat{a}-1}$. In Fig. 2a, the DCR iso-rental curves are schematically depicted, indicating which a, d combinations lead to the same number of rentals. For every a, d combination, an increase of one of the quantities always results in a higher-level curve, but the increase depends on the ratio of a and d. If a is larger than d, an increase of a causes a smaller increase of rentals r than if a and d are identical or if d is even larger than a, and vice versa.

Remark. Note that for formal reasons $A_w \leq A_z$ is required such that the matching probability does not exceed one. Naturally, $A_w \geq 0$ also holds. For $A_w > A_z$ the entire zone is always covered by the remaining available vehicles such that every arriving customer results in a rental as long as at least one vehicle is available. In this case, the matching process is rather trivial and, as we discuss later, it is covered by the ICR, the state-of-the-art matching function. This also holds for the following sections, in particular for the CCR which is discussed next.

3.3.2. The constant coverage rate matching function (CCR)

The CCR is derived from the generic matching function (1) in two steps. The first step concerns the assumption regarding the marginal coverage by an additional vehicle and, as the name suggests, the CCR assumes a constant marginal coverage. More precisely, the marginal coverage for the $(\hat{a}+1)^{st}$ vehicle is $\Delta A_{\hat{a}+1} = \min(A_z - A_{\hat{a}}, A_w \cdot \lambda)$ with $\lambda \in [0,1]$, meaning that each additional vehicle additionally covers the same fraction of the walking area $A_w \cdot \lambda$ until the residual of the zone's covered area is smaller than this $A_w \cdot \lambda$, such that the next vehicle covers this residual. The factor λ allows to formulate a constant marginal coverage which implicitly considers the potential overlap of the area covered by the individual vehicles (as for the DCR). In Appendix C, we show that for an expected number of available vehicles $\bar{a}$, for example determined by historic data, λ can be analytically approximated by

$$\lambda \approx \frac{1 - (1 - \frac{A_w}{A_z})^{\bar{a}}}{\frac{A_w}{A_z}} \cdot \frac{1}{\bar{a}}. \qquad (3)$$

With this assumption for $\Delta A_{\hat{a}+1}$, the covered area by $\hat{a}$ vehicles becomes $A_{\hat{a}} = \min(A_z, A_w \cdot \lambda \cdot \hat{a})$, and $P_{A_w,A_z}(\hat{a}) = \frac{\min(A_z, A_w \cdot \lambda \cdot \hat{a})}{A_z}$ in (1a).

In the second step to derive the CCR, the additional assumption is taken that all customers have identical matching probabilities, such that the former recursive formulation simplifies to

$$r_{A_w,A_z}(a,d) = \min\left(\frac{\min(A_z, A_w \cdot \lambda \cdot \mu \cdot a)}{A_z} \cdot d, a, d\right), \quad \forall a,d \in \mathbb{Z} \qquad (4)$$

with $\mu \in [0,1]$. The fraction in the first argument of the (outer) min()-operator in (4) represents the average matching probability for every of the d arriving customers. μ allows to formulate the average covered area $A_w \cdot \lambda \cdot \mu \cdot a$, which is a fraction of $A_w \cdot \lambda \cdot a$. In the recursive formulations, the boundary conditions ensured that rentals can not exceed a or d. In the explicit (4), this is ensured by the second and third argument of the min()-operator. (4) can be

simplified to the final CCR

$$\textbf{CCR:}\quad r^{CCR}_{A_w,A_z}(a,d) = \min\left(\frac{A_w}{A_z}\cdot\lambda\cdot\mu\cdot a\cdot d, a, d\right). \quad \forall a,d\in\mathbb{Z} \quad (5)$$

Clearly, μ has to depend on the amount of customers arriving. We show in Appendix C, that for an expected amount of customers $\bar{d}$, the parameter μ can be analytically approximated by

$$\mu \approx \frac{1}{\bar{d}}\cdot\sum_{i=1}^{\bar{d}}\left(1-\frac{A_w\cdot\lambda}{A_z}\right)^{i-1}. \quad (6)$$

Figure 1b illustrates the marginal coverage of the CCR for $\lambda=\mu=1$ and $a=3$ vehicles. Every vehicle additionally covers $A_w\cdot\lambda\cdot\mu$. In Fig. 2b, the iso-rental curves of the CCR are schematically depicted. In contrast to the DCR, for large values of a and/or d, an increase of these quantities does not result in an increase of the rentals r.

3.3.3. The infinite coverage rate matching function (ICR)

As the name suggests, the ICR assumes an infinite coverage by every additional vehicle (no friction). More precisely, the marginal coverage for the $(\hat{a}+1)^{st}$ vehicle is $\Delta A_{\hat{a}+1}=\min(A_z-A_{\hat{a}},A_z)$, meaning that the entire zone is covered as long as there is at least one vehicle available. With this assumption, $P_{A_w,A_z}(\hat{a})=1$ for every arriving customer as long as there is at least one vehicle available. Then, the ICR in dependence of a and d can be formalized by

$$\textbf{ICR:}\quad r^{ICR}_{A_w,A_z}(a,d) = r^{ICR}(a,d) = \min(a,d). \qquad \forall a,d\in\mathbb{Z} \quad (7)$$

Figure 1c illustrates the coverage of the zone according to the ICR for $a\geq 1$ vehicles, showing that the entire zone is covered. In Fig. 2c, the iso-rental curves of the ICR are schematically depicted. If a is greater or equal to d, an increase of a does not result in an increase of the rentals r, and vice versa. The iso-rental curves demonstrate that the ICR follows the characteristics of a Leontief production (Fandel, 1991, Chapter 4).

Regarding the relation between the matching functions, one can state the following: When the first argument in the min()-operator in (5) is not restrictive, the CCR (5) and the ICR (7) become identical. This first argument is not restrictive if $\lambda\cdot\mu\cdot\frac{A_w}{A_z}\cdot a\geq 1$ or $\lambda\cdot\mu\cdot\frac{A_w}{A_z}\cdot d\geq 1$. Further, the ICR is a special case of the DCR: When $A_w=A_z$, $P_{A_w,A_z}(\hat{a})=1$ for every customer in the DCR (2) such that rentals realize until all vehicles are taken, or all customers have arrived – exactly as in the ICR (7). In the schematic depiction of iso-rental curves of the DCR in Fig. 2a, the curves take the form of the ICR in Fig. 2c if $P_a=1$ for every customer. As stated in Section 3.3.1, the DCR is not defined for $A_w>A_z$. Similarly, the derivation of λ and μ for the CCR in Section 3.3.2 assumes $A_w\leq A_z$. However, more general formulations of these two matching functions that would also capture the case of $A_w>A_z$ would return rentals as for $A_w=A_z$, i.e. like the ICR, because $A_w=A_z$ already captures the case where the entire zone is covered by the available vehicles.

Remark. As discussed in Sections 1 and 2.2, it is current practice in the SMS optimization literature to determine rentals for a specific location-period combination by the minimum of the available vehicles and arriving customers (also known as "perfect/frictionless matching", see Section 2.3). Literature applies this (implicit) assumption to model both SB as well as FF SMSs. The ICR (7) is the formalization of this assumption such that the ICR could be considered as the state-of-the-art matching function, even if not discussed as such in the SMS literature. Clearly, since the ICR does not consider A_w and A_z, the ICR in general overestimates the actual matching when applied to model an FF SMS for which $A_w<A_z$. In the numerical studies in Section 4, we use the ICR as a benchmark to evaluate the DCR and CCR.

Note that in an SB SMS, where available vehicles and arriving customers refer to a specific station, the issue of overestimating rentals due to the neglection of spatial parameters A_w and A_z described above does not occur. Note further that the link between SB and FF SMSs in the context of matching modeling can be established by considering an extreme case of the zone area size: A station of an SB SMS can be considered as a zone in an FF SMS of infinitely small size – a point zone. In this point zone, the expected rentals can be correctly described by the ICR (7).

3.4. Properties

In this section, we discuss mathematical properties of the three matching functions $r^M_{A_w,A_z}(a,d)$ with $M\in\{DCR,CCR,ICR\}$. This analysis is common in the matching function literature, as it allows to assess the plausibility of the derived functions by verifying desirable properties and to analytically derive limitations of the functions' applicability. Properties 1 and 2 can be considered as standard boundary conditions for matching functions. Properties 3 and 4 are related to the special case of "perfect/ frictionless" matching (see Section 2.3) in FF SMSs. Properties 5 and 6 are specific for matching functions in FF SMSs, while especially the latter also impacts the formulation of overall optimization models for FF SMSs – a particularly relevant aspect in our work (see also Section 3.5).

Property 1 – Zero rentals boundary conditions. *If either demand or supply are zero, no rentals realize. Formally, we have* $r^M_{A_w,A_z}(a,d)=0$ *if* $a=0$ *or* $d=0$.
This property verifies an intuitive boundary condition: The absence of available vehicles or customers. Clearly, the DCR, the CCR, and the ICR fulfill this property.

Property 2 – Supply and demand limits. *If the number of available vehicles becomes infinitely large, the realized rentals equal demand, and vice versa. Formally, we have* $r^M_{A_w,A_z}(a,d)=d$ *for* $a\to\infty$ *and* $r^M_{A_w,A_z}(a,d)=a$ *for* $d\to\infty$, *respectively.*.
This property verifies an intuitive boundary condition in the abundance of available vehicles or customers. Clearly, the CCR and the ICR fulfill this property. For the DCR, consider that if $a\to\infty$, also $\hat{a}\to\infty$ and that the probability of a matching $P_{A_w,A_z}(\hat{a})=(1-(1-\frac{A_w}{A_z})^{\hat{a}})\to 1$ in (2a), for realistic parameters where $A_w\leq A_z$. If this is true for every arriving customer d, $r^M=d$. For $d\to\infty$, the recursion in (2a) is executed until all vehicles a are taken because we have $P_{A_w,A_z}(\hat{a})>0\,\forall\hat{a}>0$.

Property 3 – Matching with certainty for entire zone coverage. *If the vehicles cover the entire zone area, the next arriving customer certainly finds a vehicle and a rental results. Formally, we have* $\frac{\partial}{\partial d}r^M_{A_w,A_z}(a,d)=1$ *if* $A_a=A_z$.
This intuitive property covers constellations in which matching in an FF SMS works as matching in SB SMS. For the DCR, $A_a=A_z$ requires the special case that $A_z=A_w$, and in this case, $P_{A_w,A_z}(a)=1$ for every arriving customer, as long as there is at least one vehicle available. For the CCR, $A_a=A_z$ means that $A_w\cdot\lambda\cdot\mu\cdot a=A_z$ such that the first argument of the min()-operator is not restrictive and an additional demand results in an additional rental. The ICR fulfills this property by definition.

Property 4 – No matching for zero zone coverage. *If the vehicles cover an infinitely small zone area or the zone area grows to infinity, there is no matching. More precisely, every additional customer results in zero additional rentals. Formally, we have* $\frac{\partial}{\partial d}r^M_{A_w,A_z}(a,d)=0$ *for* $A_a\to 0$ *or* $A_z\to\infty$.
This property is the opposite of the aforementioned one. Compared to the walking distance, distances are so long that there are no rentals.

For the DCR, both of the extreme cases result in $P_{A_w,A_z}(a) \to 0$ such that an additional customer does not increase the expected rentals. For the CCR, the first argument of the min()-operator becomes zero such this property is fulfilled. The ICR does not fulfill this property and in contrast predicts an additional rental for every customer, given an available vehicle, no matter what sizes A_w and A_z take.

Property 5 – Supply and demand symmetry. *The matching function is symmetric regarding supply and demand. Formally, we have* $r^M_{A_w,A_z}(a,d) = r^M_{A_w,A_z}(d,a)$.
Obviously, the CCR and the ICR both fulfill this property. We prove symmetry of the DCR in Appendix D.

It follows from the proof, that the DCR can be formulated by interchanging $\hat{a}$ and $\hat{d}$ in (2) which yields

$$r^{DCR}_{A_w,A_z}(\hat{d},\hat{a}) = (1-(1-\frac{A_w}{A_z})^{\hat{d}}) \cdot (1 + r_{A_w,A_z}(\hat{d}-1,\hat{a}-1)) + (1-\frac{A_w}{A_z})^{\hat{d}} \cdot r^{DCR}_{A_w,A_z}(\hat{d},\hat{a}-1) \quad \forall \hat{a},\hat{d} \in \mathbb{Z} \tag{8a}$$

$$r^{DCR}_{A_w,A_z}(\hat{d},0) = 0 \qquad \forall \hat{d} \in \mathbb{Z} \tag{8b}$$

$$r^{DCR}_{A_w,A_z}(0,\hat{a}) = 0. \qquad \forall \hat{a} \in \mathbb{Z} \tag{8c}$$

The intuition of this alternative DCR formulation (8) is exactly inverse to the one described in Section 3.2.1: A customer covers a certain fraction of the zone and every part of the zone is equally likely to belong to the marginally covered area by an additional customer. The positions where the available vehicles are located are sequentially drawn at random from a uniform distribution. For each drawn vehicle, the probability that it is rented is determined by the respective proportion of the covered zone at the time it is drawn. As for the DCR formulation (2), the process ends if either the rentals realized equal the initial customer count, or if all vehicle appearances were drawn.

Property 6 – Independence to zone partitioning. *For the ICR, the expected number of rentals does not change if a homogeneous zone is artificially sub-divided into multiple sub-zones. Formally, if a zone of zone area size* $\hat{A}_z$ *is partitioned into Z sub-zones,* $r^{ICR}_{A_w,\hat{A}_z}(a,d) = Z \cdot r^{ICR}_{A_w,\hat{A}_z/Z}(\frac{a}{Z},\frac{d}{Z})$ *holds.*
Property 6 states that artificially partitioning a zone into multiple sub-zones does not change the overall expected number of rentals for the ICR. Consider that the collected data on the zone level is given by a, d, and $\hat{A}_z$. A_w is also given. When data is collected on this zone level, the only reasonable assumption is that this zone is homogeneous, such that a and d would be divided proportionally to obtain the respective quantities for the Z smaller sub-zones, i.e. $\frac{a}{Z}$ and $\frac{d}{Z}$. Consequently, the resulting rentals for the ICR in each sub-zone are the rentals of the original zone divided by Z. Since there are Z of these sub-zones, overall, the amount of rentals remains the same.

This property is the reason for the fact that the issue of inaccurate matching modeling cannot be simply solved by partitioning a zone artificially into multiple smaller sub-zones of the 'right' size for the ICR (see the corresponding statement in Section 1). This property is illustrated with a numerical example in Appendix I. Note that an analogous property holds for the DCR and CCR, which considers the probabilities of all combinations of possible discrete distributions of a and d over the sub-zones and then applies the matching functions on these sub-zones.

3.5. Integration in linear optimization problems

As described in Sections 1 and 2.2, a lot of work has been done in the literature to cover the various SMS optimization problems based on network flow modeling. Mostly, the resulting formulations are mixed-integer linear programs (MILP). As explained, our work particularly focuses on the optimization models of FF SMSss and in this section, we therefore discuss whether the introduced matching functions can be linearized *losslessly*, such that an exact integration in a typical MILP is possible.

The decisive characteristic of spatio-temporal network flow formulations, illustrated in Figure 14 in Appendix A, is a set of constraints that describe the flow conservation in the network. With discrete locations $i,j,k \in \mathcal{Z}$, and periods $t \in \mathcal{T}$, the flow conservation constraints can be formulated as

$$\sum_{i\in\mathcal{Z}} r_{ijt} + s_{jt} = \sum_{k\in\mathcal{Z}} r_{jk(t+1)} + s_{j(t+1)} \qquad \forall j \in \mathcal{Z}, t \in \mathcal{T}, \tag{9}$$

where r_{ijt} describe the rentals from location i to j in period t, and s_{jt} describe the vehicles that remain unused at location j in period t. Now, the number of rentals originating at a location i, given by $r_{it} = \sum_{j\in\mathcal{Z}} r_{ijt}$, are assumend to realize according to a specific matching function, depending on the number of available vehicles a_{it} and the arriving customers $d_{it} = \sum_{j\in\mathcal{Z}} d_{ijt}$. Therefore, the logic of the matching functions to determine r_{it} has to be formulated by means of additional constraints within the MILP formulation. Note that additional constraints are required to derive the i-j-t-specific rentals r_{ijt} from the r_{it}-values, but this is out of scope of the matching itself.

Note further that, in contrast to d_{it}, the quantities r_{it} and a_{it} are decision variables in the MILP. In certainty equivalent formulations (based on expected values), these decision variables are continuous, meaning $a_{it}, r_{it} \in \mathbb{R}^+_0 \; \forall i \in \mathcal{Z}, t \in \mathcal{T}$. In the following, we therefore discuss for each of the initial matching functions from Section 3.3, whether the range of values $\mathbb{Z}$ for a_{it} and d_{it} can be replaced by $\mathbb{R}^+_0$, how the functions are formulated for a specific i-t-combination, and whether a lossless integration in a MILP formulation is possible.

3.5.1. DCR

For a specific i-t combination, the DCR (2) becomes

$$r^{DCR}_{it,A_w,A_z}(\hat{a}_{it},\hat{d}_{it}) = (1-(1-\frac{A_w}{A_z})^{\hat{a}_{it}}) \cdot (1 + r^{DCR}_{it,A_w,A_z}(\hat{a}_{it}-1,\hat{d}_{it}-1)) + (1-\frac{A_w}{A_z})^{\hat{a}_{it}} \cdot r^{DCR}_{it,A_w,A_z}(\hat{a}_{it},\hat{d}_{it}-1) \quad \forall \hat{a}_{it},\hat{d}_{it} \in \mathbb{Z} \tag{10a}$$

$$r^{DCR}_{it,A_w,A_z}(\hat{a}_{it},0) = 0 \qquad \forall \hat{a}_{it} \in \mathbb{Z} \tag{10b}$$

$$r^{DCR}_{it,A_w,A_z}(0,\hat{d}_{it}) = 0. \qquad \forall \hat{d}_{it} \in \mathbb{Z} \tag{10c}$$

Due to the recursive formulation of the DCR (10) which is only defined for *discrete* values $\hat{a}_{it}, \hat{d}_{it} \in \mathbb{Z}$, the range of values for $\hat{a}_{it}$ and $\hat{d}_{it}$, and therewith also for $r^{DCR}_{it,A_w,A_z}(\hat{a}_{it},\hat{d}_{it})$, cannot be replaced by the *continuous* range $\mathbb{R}^+_0$. Figure 3a depicts (10) schematically (for $A_w < A_z$). For a given demand level d_{it}, it illustrates how the realized rentals $r^{DCR}_{it,A_w,A_z}(a_{it},d_{it})$ depend on the number of initially available vehicles a_{it}. Every additional vehicle increases the expected rentals with decreasing margin such that the demand is the limit of the function.

Clearly, since for a given a_{it}, d_{it}, (10) is a discrete function in $a_{it} \in \mathbb{Z} \; \forall i \in \mathcal{Z}, t \in \mathcal{T}$, the DCR can not be losslessly linearized and integrated in a MILP formulation. Note, however, that the DCR may find application in (non-linear) optimization approaches with discrete $a_{it} \in \mathbb{Z}$, such as for example in an approach based on a Markov decision process (MDP).

As for any function, an approximate linearization is possible in principle also for the DCR. However, the question is how accurate

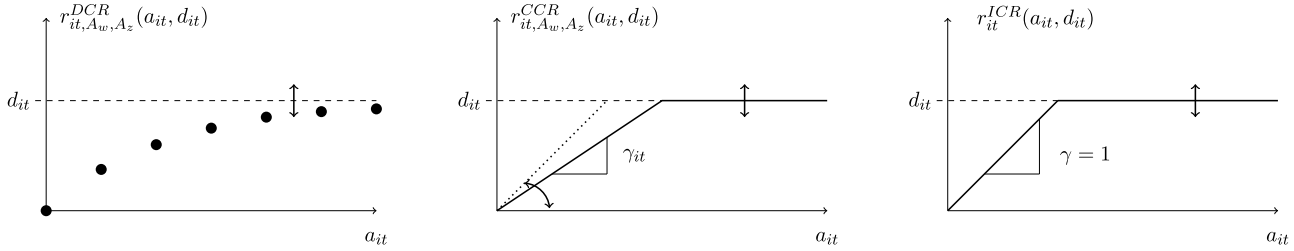

(a) DCR (10) (b) CCR (13) (c) ICR (14)

Fig. 3. Schematic representation of matching functions.

such a linearization is and, in the context of a MILP, how this impacts the number of decision variables and constraints. A reasonable way to linearize the DCR would be to define a piecewise linear function with supporting points for every $a_{it} \in \mathcal{Z}$, for which the exact r_{it} is known. This would correspond to a function that connects the dots in Fig. 3a. While this is possible in theory, it would require a large number of additional auxiliary variables in a MILP in order to determine which piece of this function is active. Thus, we do not see this as a promising path.

3.5.2. CCR

In the CCR (5), the range of values for a, d, and $r^{CCR}_{A_w,A_z}(a,d)$ can be replaced by $\mathbb{R}^+_0$. For a specific *i-t* combination, the CCR becomes

$$r^{CCR}_{it,A_w,A_z}(a_{it},d_{it}) = \min(\lambda \cdot \mu \cdot \frac{A_w}{A_z} \cdot d_{it} \cdot a_{it}, a_{it}, d_{it}). \quad \forall a_{it}, d_{it} \in \mathbb{R}^+_0 \tag{11}$$

Since λ, μ, A_w, A_z and d_{it} are parameters, one can pre-compute whether the first or the second argument of the min()-operator is smaller. We define this *i-t*-specific pre-computed parameter as

$$\gamma_{it} = \min(\lambda \cdot \mu \cdot \frac{A_w}{A_z} \cdot d_{it}, 1) \tag{12}$$

and therewith obtain

$$r^{CCR}_{it,A_w,A_z}(a_{it},d_{it}) = \min(\gamma_{it} \cdot a_{it}, d_{it}), \qquad \forall a_{it}, d_{it} \in \mathbb{R}^+_0 \tag{13}$$

which is schematically depicted in Fig. 3b. It illustrates that for the CCR (13), the number of expected rentals $r^{CCR}_{it,A_w,A_z}(a_{it},d_{it})$ is a piecewise linear function of a_{it} with two pieces, where d_{it} determines the height of the horizontal second piece. As long as $a_{it} \leq \frac{d_{it}}{\gamma_{it}}$, an increase of a_{it} results in the same marginal increase of rentals. This marginal increase is determined by the slope parameter γ_{it}, determined with (12) or tuned (based on simulations or the DCR) to obtain an overall good fit for a certain range of expected a_{it}, d_{it}. For $a_{it} > \frac{d_{it}}{\gamma_{it}}$, an increase of a_{it} does not increase $r^{CCR}_{it,A_w,A_z}(a_{it},d_{it})$.

The CCR (13) can be losslessly linearized and integrated in a MILP formulation with a set of auxiliary variables and corresponding constraints. Depending on the actual a_{it}, these constraints determine which part of the piecewise linear function needs to be active. The model (44)–(58) in Appendix F that we apply in the case study in Section 5 is an example of a CCR integrated into a MILP for a differentiated pricing optimization problem.

3.5.3. ICR

In the ICR (7), the range of values for a, d, and $r^{ICR}(a,d)$ can be replaced by $\mathbb{R}^+_0$. For a specific *i-t* combination, the ICR (7) becomes

$$r^{ICR}_{it}(a_{it},d_{it}) = \min(a_{it}, d_{it}), \qquad \forall a_{it}, d_{it} \in \mathbb{R}^+_0 \tag{14}$$

which is schematically depicted in Fig. 3c. Like for the CCR, the number of expected rentals $r^{ICR}_{it}(a_{it},d_{it})$ in the ICR is a piecewise linear function of the initially available vehicles count a_{it} with two pieces where d_{it} determines the height of the horizontal second piece. In contrast to the CCR, the slope of the first piece is $\gamma_{it} = 1$ such that every additional a_{it} results in a rental, as long as $a_{it} \leq d_{it}$.

Analogously to the CCR, a set of auxiliary variables and corresponding constraints enables a lossless integration of (14) in a MILP. Examples for the integration of the ICR in SMS optimization problems are Hardt & Bogenberger (2021) for relocation and Soppert et al. (2022) for pricing.

4. Computational study

In this section, we evaluate the rental prediction accuracy of the three matching functions DCR, CCR, and ICR introduced in Section 3.3. We consider two general settings, i.e. the *single zone single period* setting and the *multiple zones multiple periods* setting, discussed in Section 4.1 and 4.2, respectively. The subsections for each setting are organized as follows. We begin with an introduction of the setting (4.1.1 resp. 4.2.1), followed by the description of a simulation which serves as a benchmark (4.1.2 resp. 4.2.2), the parameter configurations (4.1.3 resp. 4.2.3), and the evaluation metrics (4.1.4 resp. 4.2.4). The last subsections discuss the results (4.1.5 resp. 4.2.5).

4.1. Single zone single period setting

4.1.1. Setting

The *single zone single period* (SZSP) setting is a stylized setting where the FF SMS, as the name suggests, consists of one single zone and one single period. The purpose of this setting is to isolate the assessment of the rental prediction accuracy, and to eliminate potential effects that would result from replicating a real FF SMS consisting of more than one zone and multiple periods. For each considered *parameter configuration*, characterized by a given number of available vehicles a at the beginning of the period, a given number of customers to arrive d, and a specific choice of walking area A_w and zone area A_z size, $r^M_{A_w,A_z}(a,d)$ is evaluated for the different matching functions $M \in \{DCR, CCR, ICR\}$. The outputs are compared to a benchmark from a stochastic dynamic simulation, described next.

4.1.2. Simulation benchmark

The simulation of the SZSP-setting is consistent with the generic matching process described in Section 3.2, i.e. vehicles are available at the beginning of the considered period, while customers arrive sequentially during the period. For each considered parameter configuration, we derive the benchmark by performing multiple simulation runs $n \in \mathcal{N} = \{1, 2, \ldots, N\}$ that each yield a rental observation r_n.

At the beginning of each simulation run n, a given number of available vehicles a is distributed within a squared zone of size A_z. In line with the assumptions from Section 3.2.1, a zone is homogeneous and consequently, the location of each vehicle is drawn

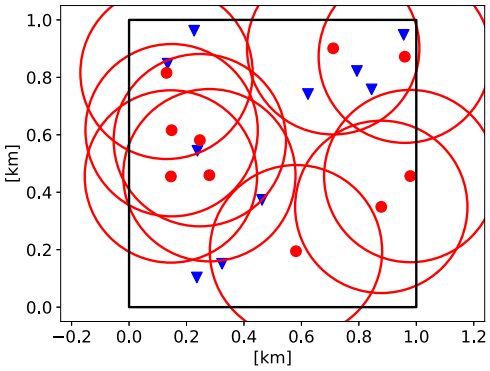

Fig. 4. Run of SZSP-scenario with $A_z = 1$ km^2 in retrospective ($a = 10$, $d = 10$).

from a uniform distribution. A given number of customers then arrive sequentially and their respective point of appearance is drawn from a uniform distribution as well. The customers have a maximum walking distance (corresponding to A_w) and the assumption is that if there is at least one vehicle within reach, the closest one is rented. This vehicle is then removed and the rental is recorded. Independent of the actual rental outcome, the number of customers to come is reduced by one and the process is repeated until all d customers have arrived. The simulation process for one simulation run is summarized as pseudo code in Algorithm 2 in Appendix E.

To clarify the setup, consider Fig. 4 that depicts a single simulation run of the SZSP-setting with $A_z = 1$ km^2 in retrospective. The $a = 10$ initially available vehicles are represented as blue triangles, and the $d = 10$ customers, that arrived sequentially during the run, are represented by red dots with their respective walking area, depicted as red circles. One of the vehicles, the one in the lower left corner of the zone, was out of reach for all customers. Consequently, this vehicle has not been rented in this simulation run. Note, however, that even though all other vehicles lay within at least one of the red circles, they were not necessarily rented, because the respective customer might have taken a different vehicle. Since Fig. 4 does not show the temporal sequence of the run, some of the vehicles depicted have not been available for the customers that arrived rather late. In fact, only $r_n = 6$ rentals realized in this particular run.

Note that Fig. 4 shows that parts of the walking area may lay outside of the zone. The actual area of the zone which is within reach of a customer therewith is smaller than the walking area. For the benchmark simulation, we exclude this effect by the following mechanism: Whenever a part of the walking area protrudes beyond the zone boundary, this part is displaced to the other side of the zone. The effect is that the entire walking area actually lies within the zone. Thus, our zone has a limited size, but effectively no border, like the surface of a sphere.

4.1.3. Parameter configurations and scenarios

We consider the following parameter settings, with every potential combination of values defining a valid parameter configuration:

- Available vehicles ($\mathcal{V}_{SZSP}$): a is selected from the discrete set $\mathcal{V}_{SZSP} = \{0, 1, \ldots, 10\}$.
- Arriving customers ($\mathcal{D}_{SZSP}$): d is selected from the discrete set $\mathcal{D}_{SZSP} = \{0, 1, \ldots, 10\}$.
- Walking area size (A_w): A_w is kept constant at $A_w = \pi \cdot (0.3\text{km})^2 = 0.28$ km^2. The radius of 0.3 km represents a realistic maximum walking distance (Herrmann et al., 2014).
- Zone area size ($\mathcal{A}_z$): A_z is selected from the discrete set $\mathcal{A}_z = \{0.5 \text{ km}^2, 1 \text{ km}^2, 2 \text{ km}^2, 4 \text{ km}^2\}$, representing the typical range of zone size values from literature (e.g. Müller et al., 2017; Weikl & Bogenberger, 2016) and practice.

We use the term SZSP-*scenario* to refer to parameter settings having the same value of A_z, i.e., we group all resulting parameter configurations for a specific A_z to belong to one scenario. Note that in this stylized setting there is no supply or demand uncertainty, meaning that a and d have no variance within a scenario but are deterministic values. We perform $N = 100$ simulation runs for every parameter setting.

4.1.4. Evaluation metrics

We use the following metrics to assess the rentals prediction accuracy:

- Rentals (RT): The expected absolute rentals RT predicted by the matching functions are simply $\bar{r} = r^M_{A_w, A_z}(a, d)$ with $M \in \{DCR, CCR, ICR\}$. With regard to the simulation benchmark, the corresponding value is obtained from averaging over the simulations runs, i.e., $\bar{r}_N = \frac{1}{N} \sum_{n \in \mathcal{N}} r_n$.
- Rentals' mean error (RT^{ME}): The mean absolute error RT^{ME} between the expected rentals $\bar{r}$ predicted by a matching function and the N observations of the simulation benchmark r_n is $RT^{ME} = \bar{r} - \bar{r}_N$.
- Rentals' mean relative error (RT^{MRE}) [%]: The mean relative error RT^{MRE} between the expected rentals $\bar{r}$ predicted by a matching function and the N observations of the simulation benchmark r_n is $RT^{MRE} = (\bar{r} - \bar{r}_N)/\bar{r}_N \cdot 100$.

4.1.5. Results

We begin by investigating the predicted and observed absolute rentals RT on an aggregate level. Therefore, we consider Fig. 5 which provides a first impression of how the different matching functions predict rentals and how the rentals observed in the simulation benchmark depend on supply, on demand, as well as on the zone area size. In each of the subfigures, the vertical axis of the surface plot represents expected and observed rentals RT for the matching functions and the simulation benchmark, respectively. The horizontal axes represent $a \in \mathcal{V}_{SZSP}$ and $d \in \mathcal{V}_{SZPZ}$, respectively. The two rows depict the results of the SZSP-scenarios $A_z = 1$ km^2 and $A_z = 2$ km^2. The respective graphs for all scenarios, i.e. for all $A_z \in \mathcal{A}_z$, are depicted in Figure 16 in Appendix G. The columns depict the mean of the simulation benchmark (SIM), and the expected rentals predicted by DCR, CCR, and ICR. From considering Fig. 5, the following observations can be made, which partly relate to the properties discussed in Section 3.4.:

- For all matching functions, the surfaces are bounded to $RT = 0$ for all a-d combinations where $a = 0$ or $d = 0$ (see Property 1). All graphs increase monotonically in a and in d, which is reasonable, since additional vehicles/ additional customers can never, ceteris paribus, decrease but may increase the (expected) rentals.
- While the surfaces of the DCR resemble the SIM benchmarks in their general shape of being strictly concave in a and d, especially the ICR but also the CCR differ as they both run into saturation if one of the inputs is fixed and the other increased (see Property 2). The ICR has the characteristic shape of a Leontief production, consisting of two planes that intersect on the diagonal between a- and d-axis. The CCR takes this shape for large values of a and d. On this a-d-diagonal, the surface of SIM and DCR is strictly concave. The ICR grows linearly on this diagonal and for the CCR, the first part of the diagonal is strictly convex and then grows linearly from some point on. For all matching functions, the surfaces are symmetric on the diagonal between a- and d-axis (see Property 5).

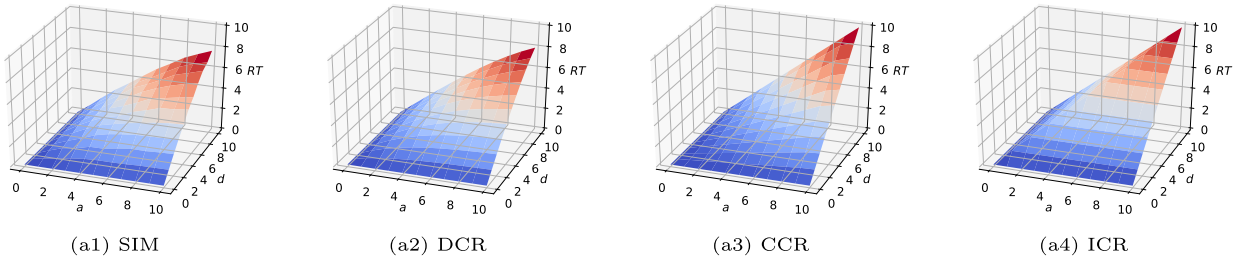

(a1) SIM (a2) DCR (a3) CCR (a4) ICR

(a) $A_z = 1$ km^2

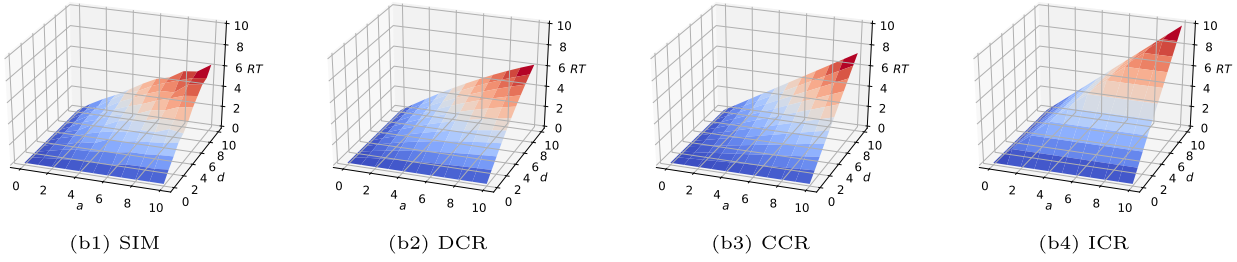

(b1) SIM (b2) DCR (b3) CCR (b4) ICR

(b) $A_z = 2$ km^2

Fig. 5. Exemplary mean (SIM) and predicted (DCR, CCR, ICR) rentals *RT* in two SZSP-scenarios.

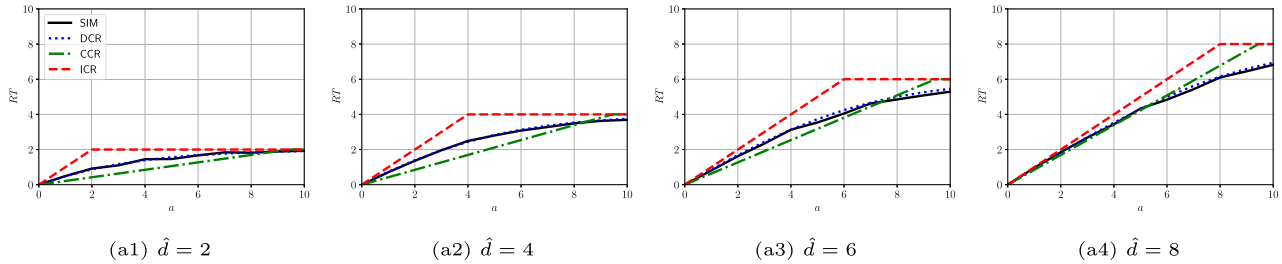

(a1) $\hat{d} = 2$ (a2) $\hat{d} = 4$ (a3) $\hat{d} = 6$ (a4) $\hat{d} = 8$

(a) $A_z = 1$ km^2

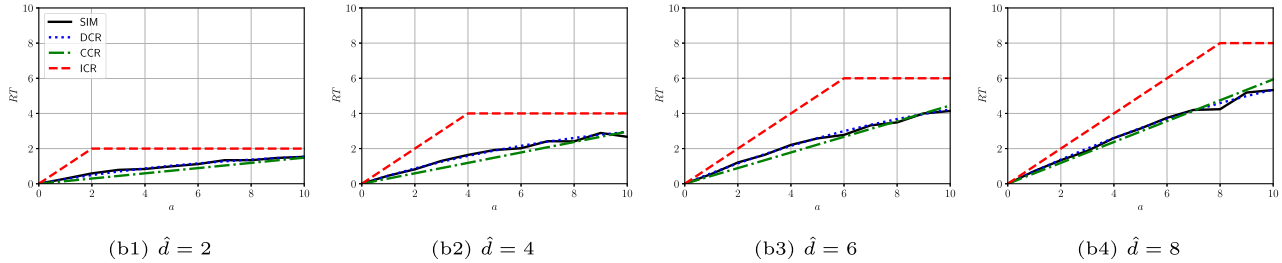

(b1) $\hat{d} = 2$ (b2) $\hat{d} = 4$ (b3) $\hat{d} = 6$ (b4) $\hat{d} = 8$

(b) $A_z = 2$ km^2

Fig. 6. Exemplary mean (SIM) and predicted (DCR, CCR, ICR) rentals *RT* in two SZSP-scenarios.

- Comparing the respective observed and predicted rentals for $a = 10$ and $d = 10$ reveals, that all matching functions overestimate the SIM results at this point, but that the DCR prediction is better than the ICR and CCR. Considering the surfaces overall, as well as the concave and convex shapes of the surfaces on the diagonal discussed above, indicates that the DCR approximates the SIM best, followed by the CCR and then the ICR.

We continue the discussion of results by comparing the rental curves *RT* for specific values of the demand $\hat{d}$, depicted in Fig. 6. These graphs which are common to depict matching functions can be thought of as corresponding vertical cuts through the surface plots in Fig. 5. Again, the two rows depict the SZSP-scenarios with $A_z = 1$ km^2 and $A_z = 2$ km^2. The respective graphs for all $A_z \in \mathcal{A}_Z$, are depicted in Figure 17 in Appendix G. The columns correspond to different demands $\hat{d}$. The simulation (SIM) results are depicted by a black solid line, the results of ICR in dashed blue, CCR in dotted red, and DCR in dotdashed green. The following observations can be made:

- As illustrated in Fig. 3 in Section 3.5, the DCR is strictly concave in a, while both ICR and CCR take the form of a piecewise linear function with a positive slope piece anchored at the origin and a second horizontal piece.

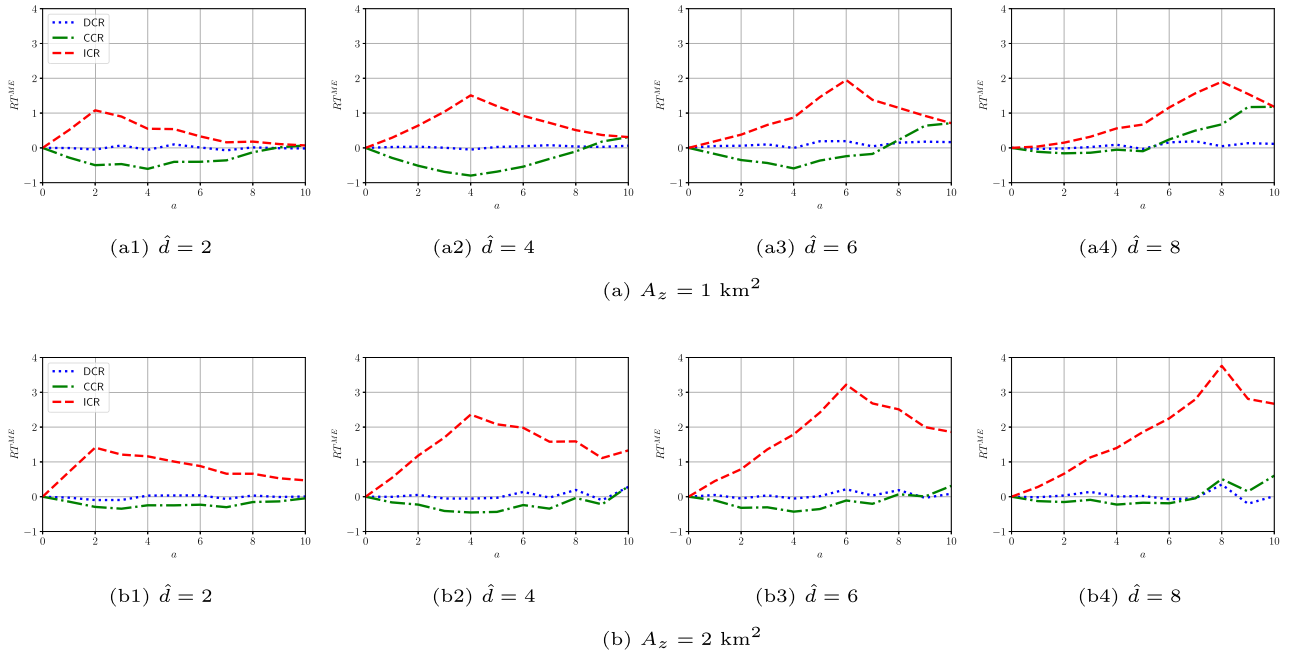

Fig. 7. Exemplary mean absolute error RT^{ME} in two SZSP-scenarios.

- The expected rentals predicted by the DCR are almost identical to the average SIM results, for all a-$\hat{d}$ combinations and all A_z. The characteristic strictly concave shape of SIM is perfectly modeled by the DCR. The CCR underestimates SIM for small values of a and $\hat{d}$. For large values, it overestimates this benchmark. As above, for large a and $\hat{d}$, the CCR and the ICR do not differ (see Figures 17(a2)-17(a4) in Appendix G).
- The ICR overestimates the SIM rentals for all a-$\hat{d}$ combinations. The difference grows in the size of the zone A_z and for a certain A_z it reaches its maximum at $a = \hat{d}$. Moreover, this maximum difference grows in $\hat{d}$. This can be explained as follows: The ICR assumes a perfect matching, which is appropriate if the zone size A_z equals the walking area. However, when the zone becomes larger, the probability that an available vehicle is actually in walking distance to a customer decreases. The maximum is at $a = \hat{d}$ because at this value, each customer needs to find a vehicle for the ICR to be exact. By contrast, imagine $d = a + 1$, then we have an additional customer and the ICR prediction is still realized if one customer cannot reach a vehicle.

In the following, we discuss the results based on the introduced metrics. Figure 7 and Table 3 in Appendix G contains the values of RT^{ME} for the DCR, CCR, and ICR for all parameter configurations, grouped by SZSP-scenarios $A_z \in \mathcal{A}_z$. The corresponding RT^{MRE} are depicted in Fig. 8 and Table 4 in Appendix G.

- For the DCR, RT^{ME} takes both positive and negative values. The minimum RT^{ME} is between -0.06 ($A_z = 0.5$ km^2) and -0.20 ($A_z = 2$ km^2), i.e. -3.8% and -1.0% RT^{MRE}. The maximum RT^{ME} is between 0.19 ($A_z = 0.5$ km^2) and 0.40 ($A_z = 1$ km^2), i.e. 2.9% and 5.6% RT^{MRE}.
- For the CCR, RT^{ME} also takes both positive and negative values. The minimum RT^{ME} is between -0.06 ($A_z = 0.5$ km^2) and -0.80 ($A_z = 1$ km^2), i.e. -13.7% and -32.0% RT^{MRE}. The maximum RT^{ME} is between 0.85 ($A_z = 0.5$ km^2) and 2.20 ($A_z = 1$ km^2), i.e. 11.9% and 28.2% RT^{MRE}.
- For the ICR, RT^{ME} only takes values greater or equal to zero. The maximum RT^{ME} is 0.85 ($A_z = 0.5$ km^2) and it grows to 5.75 ($A_z = 4$ km^2), i.e. to 11.9% and 135.3% RT^{MRE}.

The above results demonstrate that in general, the ICR matching function is not suitable to predict rentals accurately in the stylized SZSP-setting that only considers one zone. In particular, they show that only the novel matching functions are capable to adapt to different zone area sizes. While the prediction error diminishes when the zone area size equals the walking area size and might be acceptable in our scenarios with ratios of walking area and zone area in the approximate range $\frac{A_w}{A_z} \geq \frac{1}{2}$, the ICR overestimates the observed rentals in the SIM benchmark substantially for smaller $\frac{A_w}{A_z}$. Since larger zone areas are commonly used in literature as well as practice and since using multiple smaller zones comes with several disadvantages (see Section 1), the ICR's applicability is limited. In contrast, the CCR considers A_w and A_z in the matching prediction and therewith is capable of predicting the rentals in the SZSP-setting much more accurately, especially for smaller ratios of $\frac{A_w}{A_z}$. The DCR predicts the rentals best in the SZSP-setting and in particular performs better than the CCR for ratios of around $\frac{A_w}{A_z} = \frac{1}{2}$. Overall, the adaptability of CCR and DCR to different zone sizes is the key advantage over the ICR. As discussed in Section 3.5, the decisive disadvantage of the DCR is that it can not be losslessly integrated in a linear network flow SMS model, such that the DCR can not be considered in the following numerical results of the MZMP-setting.

4.2. Multiple zones multiple periods setting

4.2.1. Setting

The *multiple zones multiple periods* (MZMP) setting replicates an entire FF SMS with $Z = 59$ zones $\mathcal{Z} = \{1, 2, \ldots, Z\}$ and $T = 48$ periods $\mathcal{T} = \{0, 1, \ldots, T-1\}$ of 30 min each which together replicate one day. The purpose of this MZMP-setting is to assess how different matching functions affect the overall rental prediction accuracy when supply and demand interact in an entire FF SMS. In this setting, only the size of the zones A_z changes over the *parameter configurations*, replicating multiple FF SMSs with identical zone number but with different sizes of the operating area. Think of cities with the same number of inhabitants, but spread over areas of different sizes, i.e. with different densities. The MZMP-setting is based on a real-life FF SMS: The vehicle fleet is initially distributed

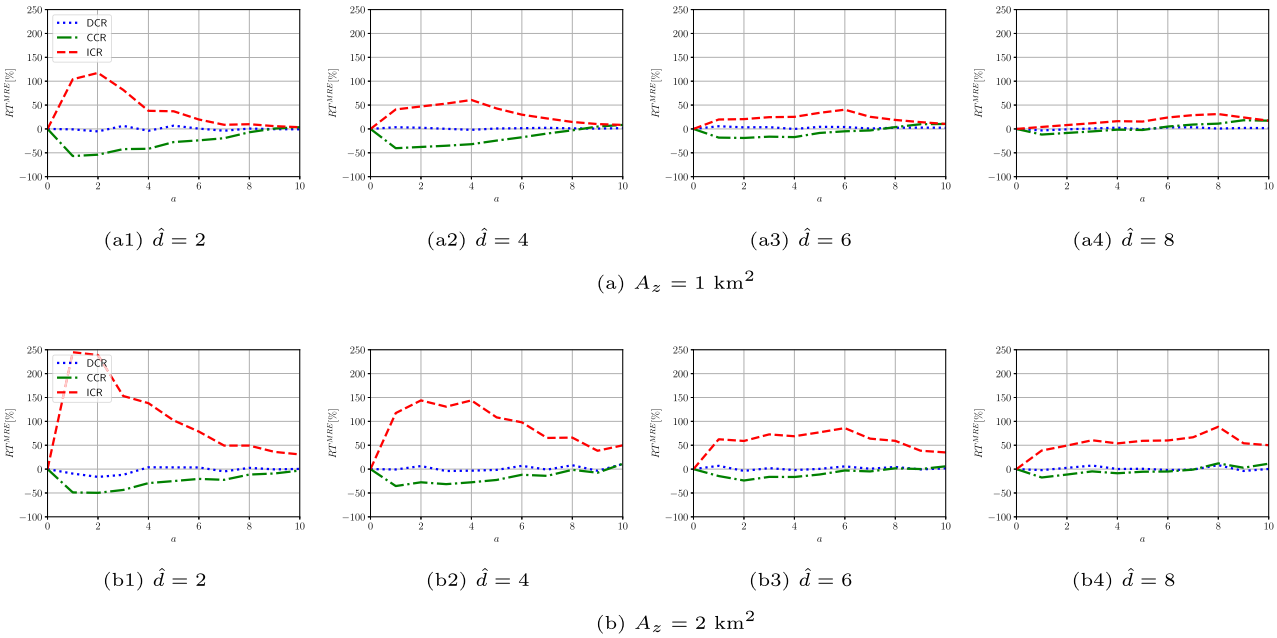

(a1) $\hat{d} = 2$ (a2) $\hat{d} = 4$ (a3) $\hat{d} = 6$ (a4) $\hat{d} = 8$

(a) $A_z = 1$ km^2

(b1) $\hat{d} = 2$ (b2) $\hat{d} = 4$ (b3) $\hat{d} = 6$ (b4) $\hat{d} = 8$

(b) $A_z = 2$ km^2

Fig. 8. Exemplary mean relative error RT^{MRE} in two SZSP-scenarios.

over the zones in line with historical data from Share Now. Customers arrive according to a demand pattern over the different zones and periods, which is obtained from historical data as well. More precisely, for every zone $i \in \mathcal{Z}$, $\hat{a}_{i0}$ defines the initial vehicle count and for every zone-zone-period combination (i-j-t combination with $i, j \in \mathcal{Z}, t \in \mathcal{T}$), the demand d_{ijt} is given.

Due to the non-disclosure agreement with our practice partner, we do not state these parameters above explicitly. However, the following general statements regarding the data used can be made. Data sources for estimating the demand are primarily the realized app openings as well as the realized rentals. Every data point of an app opening contains information regarding location and time. Clearly, not every single app opening can be counted as an individual demand, e.g. because a customer might simply check a payment history or might check vehicle availability multiple times before the actual booking. However, with much data and experience, the provider can estimate the actual demand from these app openings. These data points are then mapped to a given discretization scheme, meaning to zone-period combinations. Average values over multiple identical days can then be derived. To obtain the demand data for every zone-zone-period combination, i.e. the expected destinations for the demand originating at a certain zone-period, the proportions of rentals that realize can be used as a proxy for the demand proportions. Clearly, rentals only reflect the served (constrained) demand, which is why unconstraining techniques can come into place (see e.g. Talluri & van Ryzin, 2004, Chapter 9.4). Similar to the demand on zone-period level, the initial vehicle count can be obtained by mapping and averaging data points of available vehicles to the respective zone-period.

As in the SZSP-setting, the benchmark in the MZMP-setting stems from a stochastic dynamic simulation, with the difference that the rentals that evolve over one entire day throughout the entire SMS are considered. The latter also implies that, in contrast to the SZSP-setting, the matching functions can no longer be directly evaluated for a given parameter configuration. Therefore, to evaluate the matching functions, we integrate the two functions which can be losslessly linearized – the CCR and the ICR – in an FF SMS model that is based on a linear network flow formulation, as described in Section 3.5. In each zone-period combination, the rentals realize according to the respective matching function $r^{CCR}_{it,A_w,A_z}(a_{it}, d_{it})$ and $r^{ICR}_{it,A_w,A_z}(a_{it}, d_{it})$. The constraints of the network flow formulation ensure that these rentals r^M_{it} with $M \in \{CCR, ICR\}$ split into the different r^M_{ijt} in proportion to the given demand pattern, meaning $r^M_{ijt} = \frac{d_{ijt}}{d_{it}} \cdot r^M_{it} \; \forall i, j \in \mathcal{Z}, t \in \mathcal{T}$. Therewith, the rentals that realize over all zones and periods according to a specific matching function can be derived.

4.2.2. Simulation benchmark

For a specific parameter configuration of the MZMP-setting, we derive the respective benchmark by performing multiple simulation runs $n \in \mathcal{N} = \{1, 2, \ldots, N\}$ that each yield a rental observation $r_{ijt,n}$ for every zone-zone-period combination (i-j-t combination with $i, j \in \mathcal{Z}, t \in \mathcal{T}$). Primarily, we consider the observed rentals on the period-level, meaning $r_{t,n} = \sum_{i \in \mathcal{Z}} \sum_{j \in \mathcal{Z}} r_{ijt,n}$.

At the beginning of each run, the vehicle fleet is initialized according to the initial spatial vehicle distribution $\hat{\mathbf{a}}_0 = [\hat{a}_{i0}]_{Z \times 1}$. Each zone then exactly contains the number of vehicles as defined in $\hat{\mathbf{a}}_0$, and the precise location within a zone for each of the vehicles is randomly determined from the uniform distribution. The customer arrival process follows a Poisson process $\mathbf{P}_{\lambda_t}$ in which the intensity λ_t varies for the periods and equals the demand in the respective period, meaning $\lambda_t = \sum_{i \in \mathcal{Z}} \sum_{j \in \mathcal{Z}} d_{ijt}/30$ (unit of λ_t is [1/min]). The inter-arrival time $\Delta\tau$ until a new customer arrives is sampled from the exponential distribution $\Delta\tau \sim \text{Exp}(\lambda_t)$. Whenever a customer arrives in period t, the customer's origin zone i is determined by roulette wheel selection, i.e. the probability for arrival in i is $P^{origin}_{it} = \sum_{j \in \mathcal{Z}} d_{ijt} / \sum_{i \in \mathcal{Z}} \sum_{j \in \mathcal{Z}} d_{ijt}$ (see previous section for demand pattern d_{ijt}). The customer's exact origin location is determined by uniform distribution of positions within the origin zone. All available vehicles within the walking distance of 0.3 km are determined and, if there is at least one vehicle within reach, the customer chooses the closest one for rental. Note that, in contrast to the assumptions in the SZSP-setting (end of Section 4.1.2), customers may now cross the border of a zone and take a vehicle from a neighboring one. If there is no vehicle within reach, the customer leaves the system without further consideration. In case of a rental that originates at a certain i-t-combination, the destination zone is again determined by roulette wheel selection, i.e. the probability for destination zone j is $P^{destination}_{jt} = d_{ijt} / \sum_{k \in \mathcal{Z}} d_{ikt}$. All

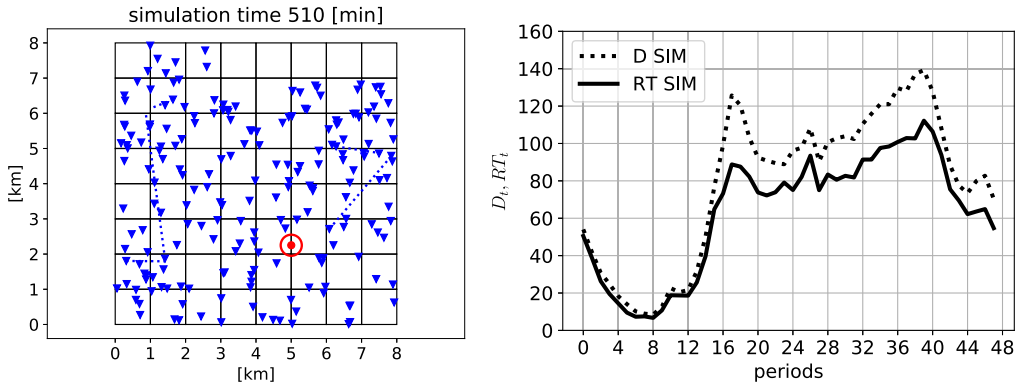

(a) Snapshot of simulation (b) Course of demand and mean rentals over periods

Fig. 9. Scenario with MZMP and $Z = 59$, $A_z = 1$ km^2, $A_o = 59$ km^2.

rentals have a duration of 15 min and immediately become available as soon as a rental is terminated. Note that here, in contrast to the SZSP-simulation, not all vehicles are necessarily available at the beginning of a period. The customer's exact destination location is determined by uniform distribution of positions within the destination zone. This process of customer arrival sampling and potential rental determination is executed until the cumulated arrival time over all customers exceeds the considered day $\tau_{\max} = 48 \cdot 30$ min. One simulation run is depicted as pseudo code in Algorithm 1.

Algorithm 1 MZMP simulation (one run $n \in \mathcal{N}$).

- initialize simulation time $\tau = 0$
- initialize rental count $r_{t,n} = 0 \; \forall t \in \mathcal{T}$
- distribute vehicles randomly according to $\hat{\mathbf{a}}_0$
- initialize set of available vehicles $\mathcal{V}^{available}$ with all vehicles
- initialize set of currently rented vehicles $\mathcal{V}^{rented} = \emptyset$

while $\tau < \tau_{\max}$ **do**
- draw inter-arrival time $\Delta\tau$ from exponential distribution $\Delta\tau \sim \text{Exp}(\lambda_t)$
- update simulation time $\tau \leftarrow \tau + \Delta\tau$
- **if** vehicles in $\mathcal{V}^{rented}$ have arrival time $< \tau$ **then**
  - remove respective vehicles from $\mathcal{V}^{rented}$
  - add respective vehicles to $\mathcal{V}^{available}$
- **end if**
- determine current period t
- determine customer's origin zone i with probabilities $P_{it}^{origin} \; \forall i \in Z$
- determine customer's exact origin location within origin zone i by uniform distribution
- determine distances to vehicles in $\mathcal{V}^{available}$
- **if** at least one vehicle in walking distance **then**
  - choose closest vehicle from $\mathcal{V}^{available}$
  - remove chosen vehicle from $\mathcal{V}^{available}$
  - add chosen vehicle to $\mathcal{V}^{rented}$
  - record rental: $r_{t,n} \leftarrow r_{t,n} + 1$
  - determine destination zone j with probabilities $P_{jt}^{destination} \; \forall j \in Z$
  - determine customer's exact destination location within j destination zone by uniform distribution
- **end if**

end while

To clarify the setup, consider Fig. 9a that depicts a snapshot of a single simulation run. In the simulation, the zones are squares of the same size and in this particular parameter configuration, $A_z = 1$ km^2 for all zones. Note that since the considered FF SMS consists of 59 zones, the five zones represented in the top row on the right are out of the simulation's scope. The vehicles are represented as blue triangles, and the currently rented vehicles are depicted at the rental origin with a dotted line that ends at the rental destination. One customer arrived in the considered instance, represented by the red dot with walking area, depicted as red circle. For this particular customer, no available vehicle was within reach. Figure 9b depicts the demand and the resulting rentals averaged over all N runs in the course of the day. More specifically, the dotted black curve represents the aggregate demand over all zones for every single period $t \in \mathcal{T}$, meaning $d_t = \sum_{i \in \mathcal{Z}} \sum_{j \in \mathcal{Z}} d_{ijt}$. The solid black curve represents the mean aggregate rentals over all zones for every single period $t \in \mathcal{T}$, meaning $\bar{r}_{t,N} = \frac{1}{N} \sum_{n \in \mathcal{N}} r_{t,N}$. This rentals curve for various parameter configurations serves as a benchmark to evaluate the rentals prediction of the matching functions qualitatively.

4.2.3. Parameter configurations and scenarios

We consider the following parameter values:

- Available vehicles ($\mathcal{V}_{MZMP}$): The initial fleet distribution $\mathcal{V}_{MZMP}$ remains constant over all studies and it is chosen according to real-life data. The overall fleet size is $\sum_{j \in \mathcal{Z}} \hat{a}_{i0} = 201$ and for the individual zones, the initial vehicle count lays in the interval $\hat{a}_{i0} \in [0, 10] \; \forall i \in \mathcal{Z}$.
- Arriving customers ($\mathcal{V}_{MZMP}$): The pattern of arriving customers $\mathcal{V}_{MZMP}$ remains constant over all studies and it is chosen according to real-life data. The d_{ijt} values vary in the interval $d_{ijt} \in [0, 18] \; \forall i, j \in \mathcal{Z}, t \in \mathcal{T}$.
- Walking area size (A_w): As in the SZSP-setting, the size of the reachable area by walking is kept constant at $A_w = \pi \cdot (0.3\text{km})^2 = 0.28$ km^2.
- Zone area size ($\mathcal{A}_z$): We obtain four scenarios by considering the sizes of the zone area $\mathcal{A}_z = \{0.5 \text{ km}^2, 1 \text{ km}^2, 2 \text{ km}^2, 4 \text{ km}^2\}$. This can be considered as *different cities* with the same fleet and demand, but spread over operating areas of *different size*, i.e. $A_o = 29.5$ km^2 to $A_o = 236$ km^2. Note that the number of zones remains identical in each scenario. In Appendix I, in contrast, we consider a setting in which a given operating area is partitioned into a different number of multiple zones.

We perform $N = 100$ simulation runs for every variant, meaning for every matching function in each parameter configuration (here equivalent to scenario).

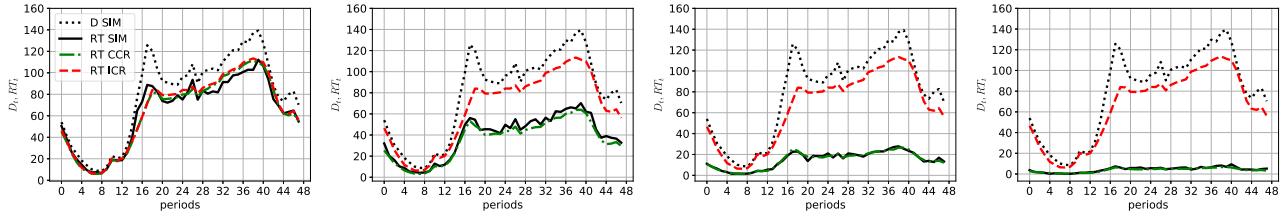

(a) $Z = 59$, $A_z = 0.5$ km^2, $A_o = 29.5$ km^2; (b) $Z = 59$, $A_z = 1$ km^2, $A_o = 59$ km^2; (c) $Z = 59$, $A_z = 2$ km^2, $A_o = 118$ km^2; (d) $Z = 59$, $A_z = 4$ km^2, $A_o = 236$ km^2

Fig. 10. Mean (SIM) and predicted (CCR, ICR) rentals RT in MZMP-scenarios with different zone and operating area sizes A_z, A_o.

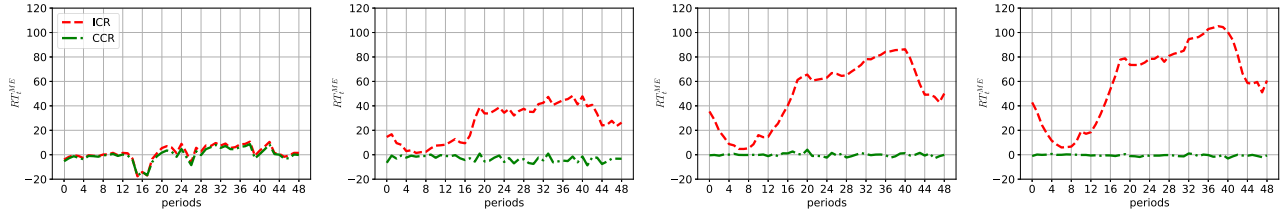

(a) $Z = 59$, $A_z = 0.5$ km^2, $A_o = 29.5$ km^2; (b) $Z = 59$, $A_z = 1$ km^2, $A_o = 59$ km^2; (c) $Z = 59$, $A_z = 2$ km^2, $A_o = 118$ km^2; (d) $Z = 59$, $A_z = 4$ km^2, $A_o = 236$ km^2

Fig. 11. Mean absolute error RT_t^{ME} in MZMP-scenarios with different zone and operating area sizes A_z, A_o.

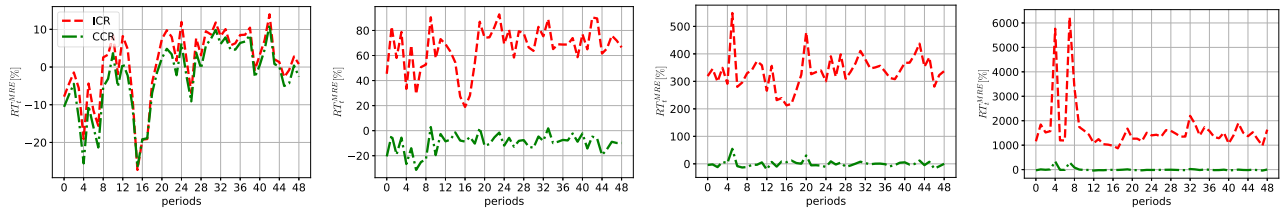

(a) $Z = 59$, $A_z = 0.5$ km^2, $A_o = 29.5$ km^2; (b) $Z = 59$, $A_z = 1$ km^2, $A_o = 59$ km^2; (c) $Z = 59$, $A_z = 2$ km^2, $A_o = 118$ km^2; (d) $Z = 59$, $A_z = 4$ km^2, $A_o = 236$ km^2

Fig. 12. Mean relative error RT_t^{MRE} in MZMP-scenarios with different zone and operating area sizes A_z, A_o.

4.2.4. Evaluation metrics

Analogous to the SZSP-setting, we use several metrics to assess the rentals prediction accuracy. Different from above, all metrics here are time-specific:

- Rentals (RT_t): The period-specific absolute rentals RT_t are determined as follows for the simulation and the matching functions. The mean observed rentals in the simulation for a specific period t are $\bar{r}_{t,N} = \frac{1}{N}\sum_{n\in\mathcal{N}}\sum_{i\in\mathcal{Z}}\sum_{j\in\mathcal{Z}} r_{ijt,n}$. The predicted rentals by the network flow-based model with integrated matching function for a specific period t are $\bar{r}_t = \sum_{i\in\mathcal{Z}}\sum_{j\in\mathcal{Z}} r_{ijt}$.
- Rentals mean error (RT_t^{ME}): The period-specific mean absolute error RT_t^{ME} between the predicted rentals by the network flow-based model with integrated matching function $\bar{r}_t$ and the mean observed rentals in the simulation $\bar{r}_{t,N}$ is $RT_t^{ME} = \bar{r}_t - \bar{r}_{t,N}$.
- Rentals mean relative error (RT_t^{MRE}) [%]: The period-specific mean relative error RT_t^{MRE} between the predicted rentals by the network flow-based model with integrated matching function $\bar{r}_t$ and the mean observed rentals in the simulation $\bar{r}_{t,N}$ is $RT^{MRE} = (\bar{r}_t - \bar{r}_{t,N})/\bar{r}_{t,N} \cdot 100$.

4.2.5. Results

Figure 10 depicts the mean rentals RT_t for the simulation benchmark (SIM) and the predicted rentals by the two linear network flow formulations with CCR and ICR in the course of the day for the four MZMP-scenarios with $A_z = 0.5$ km^2, 1 km^2, 2 km^2, and 4 km^2. In Figs. 11, 12 and Tables 5, 6 in Appendix H, the corresponding mean errors RT_t^{ME} and mean relative errors RT_t^{MRE} are depicted. The most relevant results can be summarized as follows:

- The rental curves follow the typical demand pattern with two peaks around 8:00 and 19:00.
- Despite the identical demand pattern in all scenarios, the SIM benchmark of RT_t (solid black) varies substantially. As the city considered becomes less dense (mimicked by increasing c.p. A_z), the number of rentals quickly decreases (by a factor of more than 10) from $A_z = 0.5$ km^2 to $A_z = 4$ km^2. This can be explained as follows: For small A_z (dense cities), customers' walking area is comparatively larger. This increases the matching probability because – given the same number of vehicles in the operating area – they can walk to more vehicles. By contrast, with large A_z (low density), the available vehicles are spread over large distances and customers more often do not find a vehicle in their walking distance.
- The predicted ICR rentals are identical in all scenarios, because the ICR is independent of A_z (see (7)). While for $A_z = 0.5$ km^2, the overall rental curve incidentally resembles the SIM benchmark, it increasingly overestimates the benchmark with growing A_z. Already for $A_z = 1$ km^2, the ICR rental predictions are far from the SIM benchmark. The mean error RT_t^{ME} lies between [-17.7, 10.7] for $A_z = 0.5$ km^2, [1.5, 48.2] for $A_z = 1$ km^2, [4.7, 86.3] for $A_z = 2$ km^2, and [6.0, 105.2] for $A_z = 4$ km^2. In the pe-

riods between morning and evening peak, the mean relative error RT_t^{MRE} lies in the range of [-19.3%, 14.0%] for $A_z = 0.5$ km^2, [18.9%, 92.9%] for $A_z = 1$ km^2, [21.7%, 478.7%] for $A_z = 2$ km^2, and [870.8%, 2199.6%] for $A_z = 4$ km^2.

- The CCR rentals curve resembles the the SIM benchmark for all A_z (densities). The mean error RT_t^{ME} lies between [-17.2, 8.7] for $A_z = 0.5$ km^2, [-8.7, 41.0] for $A_z = 1$ km^2, [-2.9, 4.2] for $A_z = 2$ km^2, and [-3.1, 1.0] for $A_z = 4$ km^2. In the periods between morning and evening peak, the mean relative error RT_t^{MRE} lies in the range of [-19.2%, 11.2%] for $A_z = 0.5$ km^2, [-13.7%, 2.2%] for $A_z = 1$ km^2, [-11.3%, 30.5%] for $A_z = 2$ km^2, and [-32.9%, 24.1%] for $A_z = 4$ km^2. In comparison to the ICR, the curve changes with varying zone size A_z, demonstrating the CCR's capability to adapt to scenarios with high and low density also in the MZMP-setting.

As in the SZSP-setting, also the above results in the MZMP-setting demonstrate that the ICR in general is not suitable to predict rentals accurately and that the CCR in contrast is capable of adapting to different densities. For the $A_z = 0.5$ km^2 scenario (high density), both ICR and CCR provide good rentals predictions. For larger A_z (low density), however, the ICR substantially overestimates the SIM benchmark by a factor of approximately 2 in the $A_z = 1$ km^2 scenario and up to a factor of approximately 20 in the $A_z = 4$ km^2 scenario, while the error RT_t^{MRE} of CCR remains in a relatively narrow range of up to approximately 30% at the most. It may be tempting to wrongly think that $A_z = 0.5$ km^2 always, meaning for all possible instances, is a good value for the ICR. Certainly, the results (SZSP- and MZMP-setting) show that smaller zones which are closer to the walking area are favorable over larger zones with regard to the overall rental prediction accuracy that can be obtained when applying the ICR. However, since customers and vehicles in neighboring zones do not match in network flow formulations with discrete zones (as in the MZMP-setting), rentals that realize in reality are increasingly neglected when having multiple smaller zones. This means that the increased accuracy *within* a zone might be overcompensated by a reduced accuracy *across* zones. The specific results depend on the actual homogeneity of the zones and whether they can in fact be considered as disjunct zones for which there are indeed no customers crossing the borders.

5. Pricing optimization case study

In this section, we evaluate the performance of the CCR and ICR matching functions in an FF SMS optimization problem. To that end, we present a pricing optimization case study based on Share Now data and assess whether more accurate rental predictions can result in better pricing decisions and eventually higher profits (more precisely contribution margin). The problem that we consider is a differentiated pricing problem for SMS that was discussed in Soppert et al. (2022) and for which a MILP, based on a network flow formulation, with ICR matching function was proposed. We adapt the MILP formulation by integrating the CCR. For the different instances considered in this case study, we derive pricing solutions with both of the MILP models and evaluate them in a simulation study.

The differentiated pricing problem and its original as well as the adapted mathematical modeling are introduced in Section 5.1. Section 5.2 discusses the setup of the simulation study we use to evaluate the different pricing solutions. In Section 5.3, we introduce the considered parameter configurations as well as the metrics we use. Section 5.4 discusses the obtained results.

5.1. Problem statement and mathematical modeling

The *origin-based differentiated pricing problem* (OBDPP) in SMSs, as defined in Soppert et al. (2022), is a pricing problem in which spatially and temporally differentiated minute prices have to be determined, to maximize the contribution margin of an SMS. More precisely, an SMS is discretized into Z different locations $\mathcal{Z} = \{1, 2, \ldots, Z\}$ and the considered time span of one day is discretized into T periods $\mathcal{T} = \{0, 1, \ldots, T-1\}$. For every i-t combination with $i \in \mathcal{Z}, t \in \mathcal{T}$, a minute price p_{it} is to be chosen from a given price set $\mathcal{P} = \{p^1, p^1, \ldots, p^M\}$ with corresponding price indices $\mathcal{M} = \{1, 2, \ldots, M\}$. *Origin-based* refers to the fact that, in contrast to a *trip-based* pricing mechanism for example, all rentals that begin in a certain i-t combination, are charged with the same minute price p_{it}. Note that *differentiated* (=*static*), in contrast to *dynamic* (see Agatz, Campbell, Fleischmann, Van Nunen, & Savelsbergh, 2013), refers to a pricing approach where prices do not depend on components of the current state of the system that are unobservable by the clients, such as current fleet distribution, but can be pre-computed and pre-published. The OBDPP assumes supply and demand matching according to the ICR.

The OBDPP can be modeled by a MILP which is based on a deterministic network flow formulation where expected vehicle movements are represented by flows in a spatio-temporal network, as depicted in Figure 14. Vehicle flows consist of actual rentals r_{ijt}^m from location $i \in \mathcal{Z}$ to $j \in \mathcal{Z}$ in period $t \in \mathcal{T}$ and at price p^m with index $m \in \mathcal{M}$ (solid arcs), or unused vehicles s_{it} that remain in the same location $i \in \mathcal{Z}$ at period $t \in \mathcal{T}$ (dashed arcs). For every i-j-t combination, the respective basic demand d_{ijt} is assumed to scale with the i-j-t-specific sensitivity factor f_{ijt}^m, depending on the price p^m, to the actual demand $d_{ijt}^m = d_{ijt} \cdot f_{ijt}^m$. The main components of the OBDPP MILP formulation are as follows:

- An objective function that maximizes the contribution margin from rentals that realize at different prices over the entire spatio-temporal network, meaning $\sum_{i,j \in \mathcal{Z}} \sum_{t \in \mathcal{T}} \sum_{m \in \mathcal{M}} r_{ijt}^m \cdot l_{ij} \cdot (p^m - c)$, where l_{ij} is the average rental duration and c is variable cost per minute.
- Flow conservation constraints of the form (9) as described in Section 3.5 which ensure that the fleet of vehicles remains constant in every period and that, for a certain $i-t$-combination, the available vehicles either remain unused or get rented.
- Constraints ensuring that for p_{it} exactly one of the prices from the price list $\mathcal{P}$ is chosen for every i-t-combination. If price p^m is chosen, the respective binary variable y_{it}^m is one.
- A set of constraints that determines the realization of rentals. The overall rentals for every i-t combination are determined according to the ICR. These rentals split into the i-j-t-specific rentals, proportionally according to the demand, as described in Appendix F.

The constraints in the OBDPP MILP formulation that ensure rentals realization according to the ICR can easily be replaced by corresponding constraints for the CCR. We state the resulting full MILP formulation in Appendix F. The constraints that are new compared to Soppert et al. (2022) are (49)–(54). To differentiate in the following, we denote the original problem by OBDPP-ICR and the adapted with CCR matching function by OBDPP-CCR. For solving the OBDPP-CCR, we use the decomposition solution approach described in Soppert et al. (2022) which builds on the idea to solve multiple smaller MILPs instead of the original one. The algorithm is implemented in Python 3.7 and all MILPs are solved with Gurobi 9.0.2. As in the original paper, the algorithm runs for 48 h. The simulation evaluation takes approximately 8 h without any parallelization. Given that the considered pricing problem (in Soppert et al., 2022 and, thus in this case study) is a differentiated (=static)

pricing problem, these computation times do not pose a restriction for application in practice.

5.2. Simulation evaluation

To evaluate and compare the performance of the optimization results, i.e., of the prices obtained from either optimizing using OBDPP-ICR or OBDPP-CCR, we perform a simulation study. Each run of the simulation reflects a potential real-world evolvement of the system over the considered day given the calculated pricing solutions. In essence, the simulation is in line with the one we used to calculate the simulation benchmarks for the MZMP-setting in Section 4.2.2. We only need to adapt it to allow for different prices and their effect on the demand. As described, the customer arrival process in the MZMP simulation follows a Poisson process $\mathbf{P}_{\lambda_t}$ with intensity λ_t that depends on the demand in the respective period. According to the assumption in the OBDPP, described in Section 5.1, the demand now depends on the chosen prices. Therefore, λ_t has to be calculated according to the pricing solution, meaning $\lambda_t = \sum_{i\in\mathcal{Z}}\sum_{j\in\mathcal{Z}} d^m_{ijt}/30$, where $d^m_{ijt} = d_{ijt}\cdot f^m_{ijt}$ and f^m_{ijt} depends on the price p_{it} (see Section 4.2.1 for demand pattern d_{ijt}). Accordingly, the probability for an arriving customer in period t to arrive in zone i has to be updated to $P^{origin}_{it} = \sum_{j\in\mathcal{Z}} d^m_{ijt} / \sum_{i\in\mathcal{Z}}\sum_{j\in\mathcal{Z}} d^m_{ijt}$. In case of a rental originating in a certain i-t-combination, the probability to have target zone j is $P^{destination}_{jt} = d^m_{ijt} / \sum_{k\in\mathcal{Z}} d^m_{ikt}$. Every pricing solution is evaluated with $N = 100$ simulation runs.

5.3. Parameter configurations, scenarios, and evaluation metrics

The case study builds on the MZMP-setting introduced in Section 4.2.1. The number of zones and periods, the initial vehicle distribution, and the overall demand pattern are chosen as in the MZMP-setting. Again, we consider the two scenarios with $A_z \in \{0.5\ \text{km}^2, 1\ \text{km}^2, 2\ \text{km}^2, 4\ \text{km}^2\}$ (high to low density with operating area sizes of $A_o = 29.5\ \text{km}^2$ to $A_o = 236\ \text{km}^2$). The additional parameters are chosen according to Soppert et al. (2022), that is, prices of $p^1 = 24$ cent/min, $p^2 = 30$ cent/min, $p^3 = 36$ cent/min, denoted as *low*, *base*, and *high* price. The corresponding price sensitivities are $f^1_{ijt} = 1.25$, $f^2_{ijt} = 1$, $f^3_{ijt} = 0.75\ \forall i, j \in \mathcal{Z}, t \in \mathcal{T}$ (derived from a conjoint analysis and A/B tests). Variable costs of $c = 7.5$ cent/min make up 25% of the base price. The rental time is $l_{ij} = 15$ min. Note that for these parameters, one rental realizes a contribution margin per minute of 20.625 cent/min for price p^1, 22.5 cent/min for price p^2, and 21.375 cent/min for price p^3. Thus, in a myopic optimization when there is enough supply to serve the demand, the base price p^2 would be chosen.

The results obtained by a uniform pricing with the base price, that is, without price differentiation, (BASE) serve as a benchmark for the ones by a price optimization (OPT) with OBDPP-ICR or OBDPP-CCR. In addition to the metrics defined in Section 4.2.4, we consider the following metrics:

- Relative rentals increase (RT^{rel}[%]): The RT^{rel} between rental observations with optimized pricing RT^{OPT}_n and the rental observations with base pricing RT^{BASE}_n is defined as $RT^{rel} = (\sum_{n=1}^N RT^{OPT}_n - \sum_{n=1}^N RT^{BASE}_n)/\sum_{n=1}^N RT^{BASE}_n \cdot 100$.
- Relative revenue increase (RV^{rel}[%]): The RV^{rel} between revenue observations with optimized pricing RV^{OPT}_n and revenue observations with base pricing RV^{BASE}_n is defined as $RV^{rel} = (\sum_{n=1}^N RV^{OPT}_n - \sum_{n=1}^N RV^{BASE}_n)/\sum_{n=1}^N RV^{BASE}_n \cdot 100$.
- Relative contribution margin increase (CM^{rel}[%]): The CM^{rel} between contribution margin observations with optimized pricing CM^{OPT}_n and the contribution margin observations with base pricing CM^{BASE}_n is defined as $CM^{rel} = (\sum_{n=1}^N CM^{OPT}_n - \sum_{n=1}^N CM^{BASE}_n)/\sum_{n=1}^N CM^{BASE}_n \cdot 100$.

Table 1
Simulation results of pricing solutions from OBDPP-ICR and -CCR with different $A_z \in \mathcal{A}_z$.

$A_z[\text{km}^2]$	OBDPP-	PR^{prop}_m			change w.r.t. BASE		
		low	base	high	RT^{rel}	RV^{rel}	CM^{rel}
0.5	ICR	17.1%	62.8%	20.1%	-4.3%	-0.1%	1.2%
	CCR	19.9%	61.1%	19.0%	-3.7%	0.6%	2.1%
1	ICR	17.1%	62.8%	20.1%	-3.4%	0.4%	1.6%
	CCR	34.1%	54.0%	11.1%	1.8%	3.6%	4.2%
2	ICR	17.1%	62.8%	20.1%	-3.2%	0.6%	1.8%
	CCR	16.3%	80.3%	3.5%	3.5%	4.3%	4.6%
4	ICR	17.1%	62.8%	20.1%	-5.7%	-1.9%	-0.6%
	CCR	0.0%	98.9%	1.1%	-1.3%	0.7%	1.4%

- Proportion of prices (PR^{prop}_m[%]): For a particular price p^m, the PR^{prop}_m defines the proportion of this price to all prices of a certain pricing solutions, i.e., $PR^{prop}_m = \sum_{i=1}^Z \sum_{t=0}^{T-1} y^m_{it}/(Z\cdot T)\cdot 100$.

Note that $RT^{(\cdot)}_n$, $RV^{(\cdot)}_n$, and $CM^{(\cdot)}_n$ denote the respective quantity observed in one entire simulation run, meaning the sum over all zones and periods.

5.4. Results

In Table 1, the results for the evaluated pricing solutions, generated by OBDPP-ICR and OBDPP-CCR for MZMP-scenarios with $A_z = 0.5\ \text{km}^2, 1\ \text{km}^2, 2\ \text{km}^2, 4\ \text{km}^2$ are summarized. Table 7 in Appendix H additionally depicts the corresponding confidence intervals that demonstrate the statistical significance of the respective CM^{rel} results.

- The PR^{prop}_m results for all scenarios demonstrate, that the prices in the solution obtained with the OBDPP-ICR are higher on average than those obtained with the OBDPP-CCR. For $A_z = 0.5\ \text{km}^2$, the difference in the price levels is smaller than 2 percentage points, but it grows with increasing A_z up to almost 20 percentage points for $A_z = 4\ \text{km}^2$. Exemplary, the two pricing solutions of OBDPP-ICR and OBDPP-CCR for $A_z = 2\ \text{km}^2$ are depicted in Fig. 13. Clearly, the OBDPP-ICR solution contains more high prices around the morning and evening demand peak, meaning around the periods 16 and 36. Only few of the zones, for example zone 7 and zone 49 have relatively many high prices in both solutions.
- As a consequence of the higher prices in the OBDPP-ICR solution, fewer rentals (RT^{rel}) realize in the simulation. The decrease in rentals depends on the scenario and lies between 0.6 percentage points for $A_z = 0.5\ \text{km}^2$ and to 6.7 percentage points for $A_z = 2\ \text{km}^2$.
- The revenue (RV^{rel}) obtained by the OBDPP-CCR solution is higher than the one resulting from the OBDPP-ICR in all scenarios. The gap lies in the range of 0.7 percentage points for $A_z = 0.5\ \text{km}^2$ and 3.7 percentage points for $A_z = 2\ \text{km}^2$.
- Most importantly, the contribution margin CM^{rel}, which is the objective of the pricing optimization, is significantly higher with the OBDPP-CCR pricing solution than with the OBDPP-ICR. The difference lies between 0.9 percentage points ($A_z = 0.5\ \text{km}^2$) and 2.8 ($A_z = 2\ \text{km}^2$) percentage points. Remember that for $A_z = 0.5\ \text{km}^2$, the overall rentals prediction of ICR was very accurate. The fact that even here an increase of 0.9 percentage points by using the CCR is possible shows that this coincidental overall accuracy does not necessarily translate to good decisions. First, errors at the zone level may cancel out. Second, supply and demand are endogeneous in the optimization model, and, thus, zones which have the “appropriate” parameter combination in the ICR may no longer have in the optimal solution.

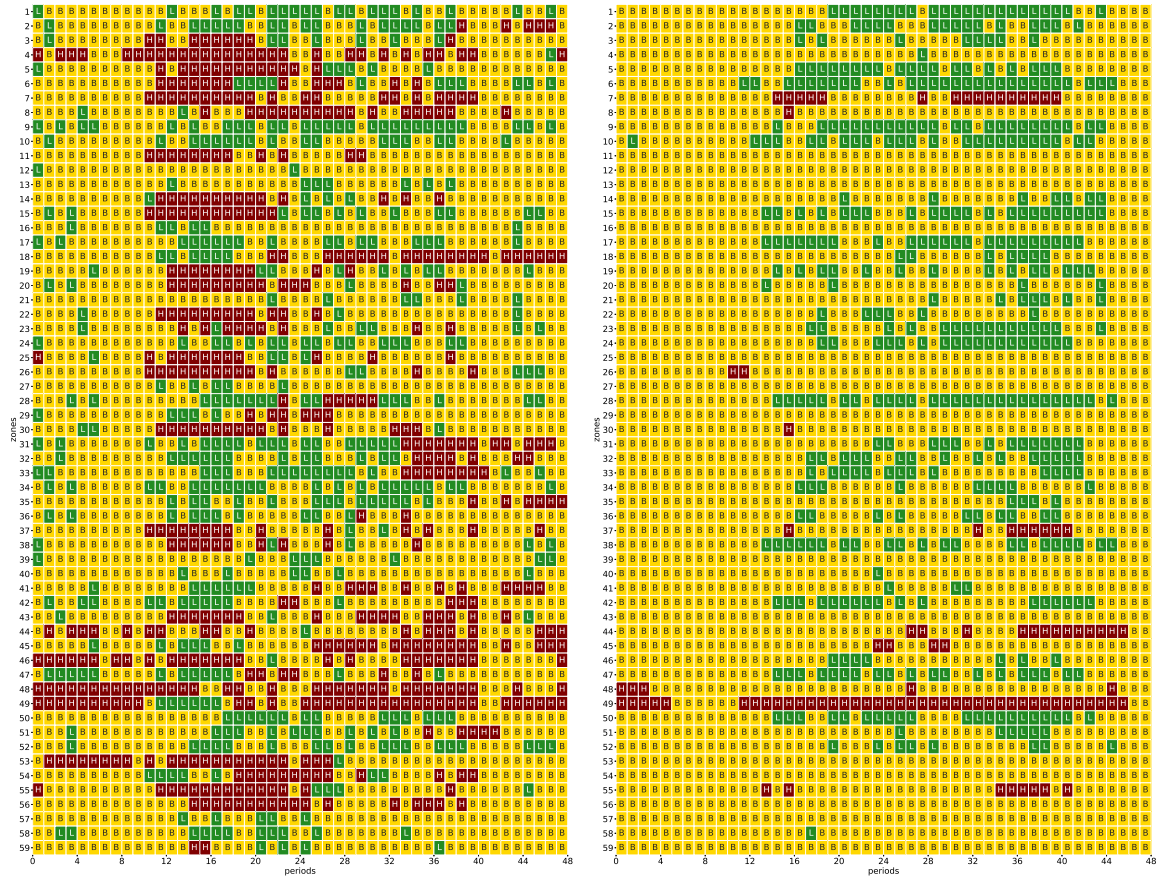

(a) OBDPP-ICR (b) OBDPP-CCR

Fig. 13. Low (L), base (B), and high (H) prices in case study scenario with $A_z = 2$ km^2.

To summarize the results of the case study, the OBDPP-CCR with improved matching modeling compared to the OBDPP-ICR yields pricing solutions that generate significantly higher contribution margins. The overestimation of rentals by the ICR causes the OBDPP-ICR to predict too many rentals in general and therewith also too many rentals when high prices are set. The optimal pricing solution according to the OBDPP-ICR therefore sets too many high prices which cause a reduction of rentals and a decrease in contribution margin when compared to the optimal pricing solution according to the OBDPP-CCR. These results demonstrate that an accurate matching modeling that considers the specific characteristics of FF SMS is highly relevant for optimizing operations. Certainly, the specific results of an instance depend on the many parameters (demand pattern, price sensitivities, etc.) but considering the results obtained in the SZSP-setting (Section 4.1), the MZMP-setting (Section 4.2) and in this case study, it seems clear that the overestimation of rentals with the OBDPP-ICR is the root cause of too high prices and the reduced profit.

6. Managerial insights and conclusion

In this paper, motivated by the insights gained in a close collaboration with Europe's largest FF car sharing provider Share Now, we examined the modeling of supply and demand matching in FF SMSs. Despite the fact that the realization of rentals is central to the accuracy of an SMS model, matching functions for SMSs have not been discussed in the literature yet and as a consequence, optimization models for SB and FF SMSs have been identical in this regard. With the development of matching functions that consider the central influencing factors specifically relevant for FF SMSs, such as customers' maximum walking distance and zone sizes, our work builds a bridge between the optimization models for SB and those for FF SMSs. This allows to adapt optimization models designed for SB to FF SMSs.

In the following, we structure the conclusions from our findings and the related managerial insights according to two central aspects, namely (1) the development and the analytical as well as computational assessment of accurate matching functions for FF SMSs and (2) the integration of the functions into FF SMS optimization approaches and the investigation of benefits that result from that.

With regard to (1), the methodological approach of developing accurate matching functions for FF SMSs was to formalize a generic, stylized matching process first and, based upon this, to systematically derive three matching functions in a second step. According to their assumptions regarding how vehicles cover the zone area, we termed the matching functions *degressive*, *constant*, and *infinite coverage rate* matching function (DCR, CCR, and ICR). While the DCR and CCR are novel matching functions, the ICR with its extremely simplified assumptions can be considered as the state-of-the-art matching function, even if not explicitly discussed as such in the SMS literature. In an extensive computational study, we compared the rental prediction accuracy by the matching functions in two settings – the first considering the rentals realization process isolated in a single zone and single period, and the second covering an entire FF SMS network consisting of multiple zones and periods.

The numerical results in the single zone single period setting revealed that the ICR in general overestimates rental: The maximum relative rental prediction errors lie in the range of 10% to

more than 100%, depending on the zone size. With the CCR and DCR, the rentals prediction is a lot more accurate: For the CCR, the relative rental prediction errors lie in the range of -30% to 30% and for the DCR in the range of -5% to 5%. In the setting with multiple zones and multiple periods, the relative rental prediction error with the ICR can (in one period) grow up to 100%-500% for medium sized and above 2000% for larger zones. For the CCR, the maximum relative rental prediction error in the relevant periods where many vehicles move lies between -15% and 30% for medium sized and between -30% and 25% for larger zones. These results support the finding that the ICR cannot accurately describe matching in an FF SMS in general and that novel matching functions, like the CCR and DCR are required.

Besides the numerical analyses, we also investigated the matching functions analytically. Most importantly, we demonstrated that only the CCR and DCR have a rentals limit value of zero when the walking distance approaches zero or the zone area grows infinitely large. This demonstrates mathematically that these two functions behave meaningfully with regard to the spatial parameters relevant in FF SMS. Among other theoretical results, we also showed analytically that the ICR is a special case of the CCR and DCR for extreme cases of large walking distance and/or small zone area size, meaning that in such situations, even the ICR could have some validity for FF SMS.

Several important insights can be concluded from these numerical and analytical results. First, to accurately describe the matching between supply and demand in an FF SMS, multiple relevant parameters have to be considered. Besides the sheer number of available vehicles and arriving customers, the zone size, the customers' maximum willingness-to-walk, successively arriving customers as well as the decreasing marginal zone coverage by additional vehicles play a decisive role. Second, the results show that only the DCR and CCR are suitable for modeling FF SMSs in general, because they do consider all of the above parameters explicitly or implicitly. The ICR in contrast has the structural problem to neglect these additionally relevant parameters and to severely overestimate rentals. Third, the necessity for more comprehensive matching functions depends on the zone sizes and the area within walking distance of the customers. All of the above insights reveal that the previously mentioned and so far unconsidered aspect of matching modeling is indeed central for managing FF SMSs and that matching modeling needs to be considered in the modeling and control of FF SMSs.

Regarding the second central aspect of our work, (2) the integration of the matching functions into FF SMS optimization approaches and the investigation of resulting benefits, we demonstrated that the CCR, opposed to the DCR, can easily be losslessly linearized. Given the vast literature on SMS optimization that use linear network flow-based formulations, this allows the adaptation of the many existing optimization approaches to be generalized such that they can be applied to both SB as well as FF SMSs. To analyze the potential benefits resulting from that, as an example, we considered a pricing optimization approach from literature in a case study based on real data from Share Now.

The numerical results from the case study show that, compared to the pricing solution with the ICR, in the pricing solution from the CCR model high prices are chosen a lot less frequently, i.e. by a factor of 20. Low prices are chosen a lot more frequently, i.e. by a factor of 2 in the CCR pricing solution, such that the different matching functions do actually impact the decision making. The better pricing decisions with the CCR cause significant contribution margin gains over the overall too high prices caused by the overestimation of rentals in the ICR pricing solution. The difference in the resulting contribution margin increase with respect to the base price benchmark was up to 3 percentage points (corresponding to an increase by factors of 1.8 to 2.6) with the pricing solution obtained by the CCR, compared to the ICR – an effect than can be solely ascribed to the more accurate matching modeling (and, thus, in a sense comes for free, compared to marketing or a fleet increase).

The main insight to derive from the pricing optimization case study is that the more accurate matching modeling of the CCR also effects the decision making in a way that benefits the overall objective. Since other FF SMS optimization problems, such as relocation or fleet sizing problems, also rely on accurate rental predictions, it is clear that they would also be affected by an overestimation of rentals. Therefore, it is a managerial task to assess the potential problem of rental overestimation based on the findings in this work and to initiate the recommended adaptations if necessary.

Taking the presented results and insights with regard to (1) and (2) into account, we believe that there are promising directions for future work. First, the consideration of *inter-zone movements* by customers as well as boundary effects at the borders of an operating area might yield improvement potential when considered in the matching modeling. Second, an *empirical study* that focuses on matching in FF SMS would have the potential to identify additional relevant factors, such as for example zone-specific characteristics like its shape or its street network. Third, it would be insightful to investigate how FF SMSs could be modeled accurately in a *spatially (and temporally) continuous* manner, with the intention to circumvent the limitations that inevitably come with the current state-of-the-art approach of spatial (and temporal) discretization. For the latter, continuous optimization techniques might be suitable. Finally, while we considered specific discretization schemes as given in our work, the complex question regarding the discretization itself is an important topic for future research.

Acknowledgements

The authors would like to thank Dr. Christian Mathissen, Head of Business Intelligence & Data Analytics at Share Now, and Dr. Alexander Baur, Team Lead Analytical Pricing & Revenue Management at Share Now, for their support, their valuable input, and the fruitful discussions within our pricing project.

Supplementary material

Supplementary material associated with this article can be found, in the online version, at doi:10.1016/j.ejor.2022.06.058.

References

Agatz, N., Campbell, A. M., Fleischmann, M., Van Nunen, J., & Savelsbergh, M. (2013). Revenue management opportunities for internet retailers. *Journal of Revenue Pricing Management, 12*(2), 128–138.

Ata, B., Barjesteh, N., & Kumar, S. (2019). Spatial pricing: An empirical analysis of taxi rides in New York City. *Working paper*. Chicago, IL: The University of Chicago Booth School of Busines.

Ataç, S., Obrenović, N., & Bierlair, M. (2021). Vehicle sharing systems: A review and a holistic management framework. *EURO Journal on Transportation and Logistics*, 100033.

Balac, M., Becker, H., Ciari, F., & Axhausen, K. W. (2019). Modeling competing free-floating carsharing operators – a case study for Zurich, Switzerland. *Transportation Research Part C: Emerging Technologies, 98*, 101–117.

Balac, M., Ciari, F., & Axhausen, K. W. (2017). Modeling the impact of parking price policy on free-floating carsharing: Case study for Zurich, Switzerland. *Transportation Research Part C: Emerging Technologies, 77*, 207–225.

Bian, B. (2018). Spatial equilibrium, search frictions and efficient regulation in the taxi industry. *Working paper*. PA: Pennsylvania State University.

Boysen, N., Briskorn, D., & Schwerdfeger, S. (2019). Matching supply and demand in a sharing economy: Classification, computational complexity, and application. *European Journal of Operational Research, 278*(2), 578–595.

Brendel, A. B., & Kolbe, L. M. (2017). Taxonomy of vehicle relocation problems in car sharing. *Working paper*. Göttingen, Germany: University of Göttingen.

Buchholz, N. (2019). Spatial equilibrium, search frictions and efficient regulation in the taxi industry. *Working paper*. Princeton, NJ: Princeton University.

Butters, G. R. (1977). Equilibrium distributions of sales and advertising prices. *The Review of Economic Studies, 44*(3), 465–491.
Ciari, F., Balac, M., & Axhausen, K. W. (2016). Modeling carsharing with the agent-based simulation MATSim: State of the art, applications, and future developments. *Transportation Research Record: Journal of the Transportation Research Board, 2564*(1), 14–20.
Ciari, F., Balac, M., & Balmer, M. (2015). Modelling the effect of different pricing schemes on free-floating carsharing travel demand: A test case for Zurich, Switzerland. *Transportation, 42*(3), 413–433.
Ciari, F., Bock, B., & Balmer, M. (2014). Modeling station-based and free-floating carsharing demand: Test case study for Berlin. *Transportation Research Record: Journal of the Transportation Research Board, 2416*(1), 37–47.
Cocca, M., Giordano, D., Mellia, M., & Vassio, L. (2019). Free floating electric car sharing design: Data driven optimisation. *Pervasive and Mobile Computing, 55*, 59–75.
Correia, G. H. D. A., & Antunes, A. P. (2012). Optimization approach to depot location and trip selection in one-way carsharing systems. *Transportation Research Part E: Logistics and Transportation Review, 48*(1), 233–247.
Data Bridge Market Research (2021). Global shared mobility market size forecast from 2021 to 2028. Statista. Accessed June 21, 2021, https://www.statista.com/statistics/1229457/shared-mobility-market-size-worldwide/.
DeMaio, P. (2009). Bike-sharing: History, impacts, models of provision, and future. *Journal of Public Transportation, 12*(4), 41–56.
Fandel, G. (1991). *Theory of production and cost*. Berlin, Germany: Springer.
Ferrero, F., Perboli, G., Vesco, A., Caiati, V., & Gobbato, L. (2015a). Car-sharing services – Part A taxonomy and annotated review. *Working paper*. Turin, Italy: Istituto Superiore Mario Boella.
Ferrero, F., Perboli, G., Vesco, A., Musso, S., & Pacifici, A. (2015b). Car-sharing services – Part B business and service models. *Working paper*. Turin, Italy: Istituto Superiore Mario Boella.
Fishman, E., Washington, S., & Haworth, N. (2013). Bike share: A synthesis of the literature. *Transport Reviews, 33*(2), 148–165.
Fréchette, G., Lizzeri, A., & Salz, T. (2018). Frictions in a competitive, regulated market evidence from taxis. *Working paper*. Cambridge, MA: National Bureau of Economic Research.
Golalikhani, M., Oliveira, B. B., Carravilla, M. A., Oliveira, J. F., & Antunes, A. P. (2021a). Carsharing: A review of academic literature and business practices toward an integrated decision-support framework. *Transportation Research Part E: Logistics and Transportation Review, 149*.
Golalikhani, M., Oliveira, B. B., Carravilla, M. A., Oliveira, J. F., & Pisinger, D. (2021). Understanding carsharing: A review of managerial practices towards relevant research insights. *Research in Transportation Business & Management*.
Haider, Z., Nikolaev, A., Kang, J. E., & Kwon, C. (2018). Inventory rebalancing through pricing in public bike sharing systems. *European Journal of Operational Research, 270*(1), 103–117.
Hall, R. E. (1979). A theory of the nature of the natural unemployment rate. *Journal of Monetary Economics, 5*(2), 153–169.
Hardt, C. (2018). Empirical analysis of demand patterns and availability in free-floating carsharing systems. *2018 21st International conference on intelligent transportation systems (ITSC)*, 1186–1193.
Hardt, C., & Bogenberger, K. (2021). Dynamic pricing in free-floating carsharing systems - a model predictive control approach. *TRB 100th Annual meeting compendium of papers*.
Heilig, M., Mallig, N., Schröder, O., Kagerbauer, M., & Vortisch, P. (2018). Implementation of free-floating and station-based carsharing in an agent-based travel demand model. *Travel Behaviour and Society, 12*, 151–158.
Herrmann, S., Schulte, F., & Voß, S. (2014). Increasing acceptance of free-floating car sharing systems using smart relocation strategies: A survey based study of car2go hamburg. In *Computational logistics. ICCL 2014. Lecture notes in computer science: vol. 8760* (pp. 151–162). London: Springer.
Illgen, S., & Höck, M. (2019). Literature review of the vehicle relocation problem in one-way car sharing networks. *Transportation Research Part B: Methodological, 120*, 193–204.
Jorge, D., & Correia, G. H. D. A. (2013). Carsharing systems demand estimation and defined operations: A literature review. *European Journal of Transport Infrastructure Research, 13*(3), 201–220.
Jorge, D., Molnar, G., & Correia, G. H. D. A. (2015). Trip pricing of one-way station-based carsharing networks with zone and time of day price variations. *Transportation Research Part B: Methodological, 81*, 461–482.
Laporte, G., Meunier, F., & Wolfler Calvo, R. (2015). Shared mobility systems. *4OR, 13*(4), 341–360.
Laporte, G., Meunier, F., & Wolfler Calvo, R. (2018). Shared mobility sytems: An updated survey. *Annals of Operations Research, 271*(1), 105–126.
Li, Q., Liao, F., Timmermans, H. J., Huang, H., & Zhou, J. (2018). Incorporating free-floating car-sharing into an activity-based dynamic user equilibrium model: A demand-side model. *Transportation Research Part B: Methodological, 107*(1), 102–123.
Lippoldt, K., Niels, T., & Bogenberger, K. (2019). Analyzing the potential of user-based relocations on a free-floating carsharing system in cologne. *Transportation Research Procedia, 37*(9), 147–154.
Lu, M., Chen, Z., & Shen, S. (2017). Optimizing the profitability and quality of service in carshare systems under demand uncertainty. *Available at SSRN*.
Lu, R., Correia, G., Zhao, X., Liang, X., & Lv, Y. (2021). Performance of one-way carsharing systems under combined strategy of pricing and relocations. *Transportmetrica B, 9*(1), 134–152.
Manley, D. (2019). Scale, aggregation, and the modifiable areal unit problem. In M. Fischer, & P. Nijkamp (Eds.), *Handbook of regional sci* (pp. 1–15). Berlin: Springer.
Molnar, G., & Correia, G. H. D. A. (2019). Long-term vehicle reservations in one-way free-floating carsharing systems: A variable quality of service model. *Transportation Research Part C: Emerging Technologies, 98*(1), 298–322.
Müller, J., Correia, G. H. D. A., & Bogenberger, K. (2017). An explanatory model approach for the spatial distribution of free-floating carsharing bookings: A case-study of German cities. *Sustainability, 9*(7), 1290.
Neijmeijer, N., Schulte, F., Tierney, K., Polinder, H., & Negenborn, R. R. (2020). Dynamic pricing for user-based rebalancing in free-floating vehicle sharing: A real-world case. *International conference on computational logistics*, 443–456.
Niels, T., & Bogenberger, K. (2017). Booking behavior of free-floating carsharing users. *Transportation Research Record: Journal of the Transportation Research Board, 2650*(1), 123–132.
Petrongolo, B., & Pissarides, C. A. (2001). Looking into the black box: A survey of the matching function. *Journal of Economic Literature, 39*(2), 390–431.
Reiss, S., & Bogenberger, K. (2016). Optimal bike fleet management by smart relocation methods: Combining an operator-based with an user-based relocation strategy. *IEEE International Conference on Intelligent Transportation Systems (ITSC)*, 2613–2618.
Ricci, M. (2015). Bike sharing: A review of evidence on impacts and processes of implementation and operation. *Research in Transportation Business & Management, 15*, 28–38.
Shaheen, S., Cohen, A., & Jaffee, M. (2018). *Innovative mobility: Carsharing outlook*. Berkeley, CA: Technical Report, Transportation Sustainability Research Center University of California.
Shaheen, S., Sperling, D., & Wagner, C. (1998). Carsharing in Europe and North American: Past, present, and future. *Transportation Quarterly, 52*(3), 35–52.
Share Now (2021). Overview on countries and cities. share-now.com, Accessed June 21, 2021, https://www.share-now.com/de/en/country-list/.
Soppert, M., Steinhardt, C., Müller, C., & Gönsch, J. (2022). Differentiated pricing of shared mobility systems considering network effects. *Transportation Science*. https://doi.org/10.1287/trsc.2022.1131. ePub ahead of print April 1.
Talluri, K. T., & van Ryzin, G. J. (2004). *The theory and practice of revenue management*. Boston, MA: Springer.
Weikl, S., & Bogenberger, K. (2013). Relocation strategies and algorithms for free-floating car sharing systems. *IEEE Intelligent Transportation Systems Magazine, 5*(4), 100–111.
Weikl, S., & Bogenberger, K. (2015). A practice-ready relocation model for free-floating carsharing systems with electric vehicles – mesoscopic approach and field trial results. *Transportation Research Part C: Emerging Technologies, 57*, 206–223.
Weikl, S., & Bogenberger, K. (2016). Integrated relocation model for free-floating carsharing systems. *Transportation Research Record: Journal of the Transportation Research Board, 2563*(1), 19–27.
Wu, C., Le Vine, S., Sivakumar, A., & Polak, J. (2019). Traveller preferences for free-floating carsharing vehicle allocation mechanisms. *Transportation Research Part C: Emerging Technologies, 102*, 1–19.
Yan, C., Zhu, H., Korolko, N., & Woodard, D. (2020). Dynamic pricing and matching in ride-hailing platforms. *Naval Research Logistics, 67*, 705–724.